Richards Tests

Andy Wilkins
CSIRO

June 5, 2014

Contents

1 Introduction

The Richards' equation describes slow fluid flow through a porous medium. This document describes the test suite associated with the Richards MOOSE code: both brief unit-style tests, and more complicated benchmark verifications. Many of the tests are run automatically every time the code is updated. Some of the tests are marked 'heavy' since they are more lengthy (they take over 2 seconds to run) and these must be run manually. There are two other accompanying documents: (1) The theoretical and numerical foundations of the code, which also describes the notation used throughout this document; (2) Examples of input syntax that users can utilise when building models.

The test suite does not *prove* that the Richards' equation is correctly implemented in MOOSE, as the expected results might be obtained by pure luck. At present around 90% of C++ code are covered by the tests, with much of the remainder being exception catching in object constructors (checking user input is correctly formatted, etc). The tests are ordered approximately by complexity, so that by the end I hope that all readers will agree that the implementation is highly likely to be correct. The tests are as follows.

- Chapter 2 tests the so-called UserObjects that define the Richards' nonlinear functions: relative permeability, density, and effective saturation. These functions are independent of the Darcy/Richards flow, but of course they must be correctly implemented in order that the code give correct solutions of flow problems.
- Chapter 3 contains many tests the Jacobian of Richards' flow. The Jacobian actually has little effect on the final numerical solution of a flow problem, but if it is incorrectly implemented then MOOSE will display poor convergence characteristics. Therefore it is extremely important to check the Jacobian.
- Chapter 4 checks that the fluid mass is calculated correctly.
- Chapter 5 contains many tests of the long-time behaviour in simple problems, which should just be hydrostatic pressure head, with the caveat that $S \geq S_{\rm imm}$.
- Chapter 6 checks that the piecewise-linear sink and the half-Gaussian sink are implemented correctly.
- Chapter 7 checks that the piecewise-linear stream-type sink (the PolyLineSink) is implemented correctly.
- Chapter 8 checks that pressure pulses diffuse correctly through a fully-saturated medium.
- Chapter 9 checks that MOOSE behaves correctly when the system contains a sink flux that is a function of porepressure. A particular function is used so that an analytic solution exists.

- Chapter 10 compares MOOSE with the Theis solution for extraction of fluid from a saturated aquifer.
- Chapter 11 demonstrates that boreholes are correctly implemented by comparing with the desired expression for the flux to the borehole, and by comparing with the known 2D analytic solution.
- Chapter 12 demonstrates that flow in the unsaturated region along with source fluxes is correctly implemented by comparing with the analytic solution of Broadbridge and White for constant infiltration.
- Chapter 13 demonstrates that flow in the unsaturated region is correctly implemented by comparing with the analytic solution of Warrick, Lomen and Islas for drainage of a medium under the action of gravity.
- Chapter 14 compares MOOSE with numerical results from HYDRUS for infiltration and drainage from a large caisson. In reality, this is very similar to Chapters 12 and 13: the only essential differences are the capillary and relative permeability functions.
- Chapter 15 compares a single-phase MOOSE simulation with the analytic solution of the Buckley-Leverett problem.
- Chapter 16 demonstrates that MOOSE yields the expected answer for a simulation containing an excavation.
- Chapter 17 compares a two-phase MOOSE simulation with the analytic solution of water infiltration provided by Rogers, Stallybrass and Clements.
- Chapter 18 compares a two-phase MOOSE simulation with the analytic solution of the Buckley-Leverett problem.

2 UserObject tests

The Richards' UserObjects define the nonlinear functions that form the core of all models. The tests of these UserObjects involve checking whether the functions and their derivatives are correctly coded. This is done by comparing the values of the UserObjects with ParsedFunctions that are coded into a MOOSE input file, and the values of the UserObject derivatives with finite-differences of the same ParsedFunction. These are simple tests and are part of the automatic test suite. The following tests are performed.

- That the 'power' form of the relative permeability:

$$\kappa_{\rm rel}(S) = (n+1)S^n - nS^{n+1} \ , \tag{2.1}$$

  is correctly coded, and also that its first and second derivatives with repsect to S are correctly coded.

- That the 'van Genuchten' form of the relative permeability:

$$\kappa_{\rm rel}(S) = \sqrt{S}\left(1-\left(1-S^{1/m}\right)^m\right)^2 \ , \tag{2.2}$$

  is correctly coded, and also that its first and second derivatives with respect to S are correctly coded.

- That the 'modified van Genuchten' form of the relative permeability:

$$\kappa_{\rm rel}(S) = \begin{cases} \sqrt{S}\left(1-\left(1-S^{1/m}\right)^m\right)^2 & \text{for } S < S_{\rm cut} \\ \text{cubic} & \text{for } S \geq S_{\rm cut} \end{cases} \tag{2.3}$$

  is correctly coded, and also that its first and second derivatives with respect to S are correctly coded.

- That the 'Broadbridge-White' form of the relative permeability:

$$\kappa_{\rm rel}(S) = \kappa_n + (\kappa_s - \kappa_n)\frac{\Theta^2(C-1)}{C-\Theta} \ , \tag{2.4}$$

  where $\Theta = (S-S_n)/(S_s-S_n)$, is correctly coded, and also that its first and second derivatives with respect to S are correctly coded. Broadbridge and White assume that saturation is bounded $S_n \leq S \leq S_s$, so for most MOOSE models it is appropriate to treat S_n as the immobile saturation with $\kappa_n = 0$, and $S_s = 1$ with $\kappa_s = 1$.

- That the 'monomial' form of the relative permeability:

$$\kappa_{\rm rel}(S) = S^n \ , \tag{2.5}$$

is correctly coded, and also that its first and second derivatives with repsect to S are correctly coded.

- That the 'powergas' form of the relative permeability:

$$\kappa_{\rm rel}(S) = 1-(n+1)(1-S)^n + n(1-S)^{n+1} \ , \tag{2.6}$$

is correctly coded, and also that its first and second derivatives with repsect to S are correctly coded.

- That the 'constant bulk modulus' form of the density

$$\rho(P) = \rho_0 e^{P/B} \ , \tag{2.7}$$

is correctly coded, and also that its first and second derivatives with respect to P are correctly coded.

- That the 'ideal gas' form of the density

$$\rho(P) = s(P-P_0) \ , \tag{2.8}$$

is correctly coded, and also that its first and second derivatives with respect to P are correctly coded.

- That the density of methane (kg.m^{-3}) at 20degC as a function of P (Pa) for pressures less than 12 MPa:

$$\rho(P) = 6.54576947608 \times 10^{-6} P + 1.04357716547 \times 10^{-13} P^2 \tag{2.9}$$

is correctly coded, and also that its first and second derivatives with respect to P are correctly coded.

- That the 'van Genuchten' effective saturation

$$S_{\rm eff} = \left(1 + (\alpha P_{\rm c})^{\frac{1}{1-m}}\right)^{-m} \ , \tag{2.10}$$

is correctly coded, and also that its first and second derivatives with respect to $P_{\rm c}$ are correctly coded.

- That the 'Broadbridge-White' effective saturation valid for small κ_n, defined by

$$\frac{P_{\rm c}}{\lambda_s} = \frac{1-\Theta}{\Theta} - \frac{1}{C}\log\left(\frac{C-\Theta}{(C-1)\Theta}\right) \ , \tag{2.11}$$

with $\Theta = (S_{\rm eff} - S_n)/(S_s - S_n)$, is correctly coded, and also that the first and second derivatives of $S_{\rm eff}$ with respect to $P_{\rm c}$ are correctly coded. Note that Broadbridge and White assume that $S_{\rm eff} = S$ (no residual saturations) and $S_n \le S \le S_s$, so in most MOOSE models S_n is the immobile saturation.

- That the ‘Rogers-Stallybrass-Clements’ effective saturation, valid for zero residual saturations and oil viscosity double that of water viscosity, defined by

$$S_{\text{eff}} = \frac{1}{\sqrt{1+\exp\left(\frac{P_{\text{c}}-P_{\text{shift}}}{P_{\text{scale}}}\right)}}\,, \tag{2.12}$$

  and its derivatives with respect to P_{c} are correctly coded.

3 Jacobian tests

The UserObjects and their derivatives need to be combined to form a residual and a Jacobian during the solution process. Correctly coding the Jacobian leads to rapid convergence to the correct solution, so tests of the Jacobian are important. These are simple tests and are part of the automatic test suite.

In MOOSE parlance, the Jacobian consists of 'Diagonal' and 'OffDiagonal' terms. The former consist of the derivative of a variable's residual with respect to the same variable (at the same quadrature point or a different one); while the latter consist of the derivatives with respect to another variable (at the same quadrature point or a different one).

The 'Diagonal' terms are tested using a single-phase single-element model with random initial conditions. Twenty four different tests are performed which are all possible combinations of:

- Fully-saturated or unsaturated initial conditions
- With or without gravity
- Without upwinding, or with SUPG, or with full upwinding
- With or without unlumped time derivatives

Of course, the unsaturated cases with gravity, SUPG/full-upwinding and time derivatives are the most complicated, but the other cases are useful for debugging. In addition, the Jacobian of the lumped time derivative is checked.

The 'OffDiagonal' terms only appear if there is more than one pressure variable, that is for multi-phase problems. A two-phase single-element model is used with random initial conditions obeying the constraint $P_1 \geq P_2$ (to be meaningful physically). Twelve different tests are performed which model all possible combinations of:

- With or without gravity
- Without upwinding, or with SUPG, or with full upwinding
- With or without unlumped time derivatives

Two other tests also performed: the first with random initial conditions subject to $P_1 = P_2$ so that the system is fully saturated with the "1" phase; and the second with random initial conditions subject to $P_1 \ll P_2$ so the system is almost fully saturated with the "2" phase.

In addition to these tests, a lumped time derivative is used in three two-phase tests: with gravity and SUPG; with gravity, SUPG and fully saturated with the "1" phase; with gravity and SUPG and almost fully saturated with the "2" phase.

In addition to these tests, two two-phase tests are performed with a fully-upwind flux: fully saturated with the “1” phase; with gravity and SUPG and almost fully saturated with the “2” phase.

In addition to these tests, the Jacobians for the following sinks/sources are tested:

- Piecewise linear sink, with and without full upwinding, with and without mobility terms in the flux
- Half Gaussian sink
- Polyline stream sink

4 Fluid mass

The total fluid mass within a volume V is

$$\int_V \phi \rho S \, . \tag{4.1}$$

It must be checked that MOOSE calculates this correctly in order that mass-balances be correct, and also because this quantity is used in a number of tests below.

A 1D model with $-1 \leq x \leq 1$, and with two elements of size 1 is created with the following properties:

Constant fluid bulk modulus	1 Pa
Fluid density at zero pressure	1 kg.m^{-3}
Residual fluid saturation	0.1
Residual air saturation	0.1
Van Genuchten m	0.5
Van Genuchten α	1 Pa^{-1}
Porosity	0.1

The porepressure is set at $P = x$.

For linear-lagrange elements, MOOSE calculates the integral over $-1 \leq x \leq 1$ by performing a sum over quadrature points at $x = \pm 0.788675$ and $x = \pm 0.211325$. Using the properties given above, this yields:

x	p	Density	S_{eff}	Saturation	Mass
-0.788675	-0.788675	0.454447	0.785188	0.72815	0.016545
-0.211325	-0.211325	0.809511	0.978392	0.882714	0.035728
0.211325	0.211325	1.235314	1	0.9	0.055589
0.788675	0.788675	2.200479	1	0.9	0.099022
				Total	0.206884

MOOSE also gives the total mass as 0.206884 kg. This test is part of the automatic test suite that is run every time the code is updated.

Since the same computer code is used for single and multi phase simulations, the fluid mass does not need to be checked for anything other than the single-phase case.

5 Long-time behaviour

These tests concern the steadystate pressure distribution obtained either by running a transient model for a long time, or by running a steady-state analysis, both of which should lead to the same result. Without fluxes, the steadystate pressure distribution is just

$$P(x) = P_0 - \rho_0 g x \ , \tag{5.1}$$

if the fluid bulk modulus, B, is large enough compared with P, otherwise

$$P(x) = -B \log \left(e^{-P_0/B} + \frac{g\rho_0 x}{B} \right) \ . \tag{5.2}$$

Here I am assuming the density is given by $\rho = \rho_0 e^{-P/B}$ with constant bulk modulus, g is the magnitude acceleration due to gravity (a vector assumed to be pointing in the negative x direction), and x is position. The tests described below are simple tests and are part of the automatic test suite.

This is verified by running twenty four single-phase single-element models with random initial conditions. The twenty four cases are combinations of:

- Fully-saturated or unsaturated initial conditions
- With or without gravity
- Without upwinding, or with SUPG, or with full upwinding
- Transient or Steadystate

Twelve two-phase simulations are also run. These are also single-element models, but with initial conditions that ensure the saturations of the phases are between 0.3 and 0.7. These twelve cases are combinations of:

- With or without gravity
- Without upwinding, or with SUPG, or with full upwinding
- Transient or Steadystate

A test with gravity and SUPG using the lumped time derivative is also run. In the two-phase situation, Eqn (5.2) must hold for each phase, and the constant P_0 for each phase is determined through conservation of mass of each phase. (In the steadystate situation, conservation of mass is meaningless, so P_0 is arbitrary, but Eqn (5.2) must still hold.)
In addition to these cases, a number of more complicated scenarios are also part of the automatic test suite:

1. A single-phase situation with nonzero immobile saturation. There are 5 elements in the x direction along which gravity acts. The x direction has length 20 m, and the initial condition is sufficiently unsaturated so that after some time the saturation at the 'top' of the model ($x \sim 20$) would reduce below immobile saturation if the relative permeability weren't preventing it. Three cases are studied: without upwinding, with SUPG, and with full upwinding. The results are shown in the top two pictures of Figure 5.1 and show that SUPG reduces oscillations and prevents $S < S_{\rm imm}$ in this example at least, while full upwinding gives exactly the desired result.

2. The same situation is in item 1, but with 50 elements in the x direction. Figure 5.1 shows once again the upwinding, as well as the hydrostatic pressure head for $S > S_{\rm imm}$. The differences between no upwinding, SUPG and full upwinding become small.

3. A two-phase situation that starts with $P_1 = P_2$, that is fully saturated. A single element is used, along with gravity, SUPG, and transient analysis. Four simulations are performed:

   a) with an unlumped time derivative
   b) with a lumped time derivative
   c) with full upwinding
   d) using a `RichardsMultiphaseProblem` object to maintain the bound $P_2 \geq P_1$.

   These simulations check that the MOOSE implementation yields the correct long-time behaviour for fully-saturated two-phase simulations.

4. A two-phase simulation with nonzero immobile saturations for both phases. Both the unlumped time derivative and lumped time derivative are tested, as well as full upwinding. The automatic test suite contains 20-element versions, and the results are shown in Figure 5.2, along with the results from a 200-element version. These figures demonstrates the reduction in spurious oscillations obtained by using a lumped time derivative, but illustrates the advantage of using full upwinding in such problems.

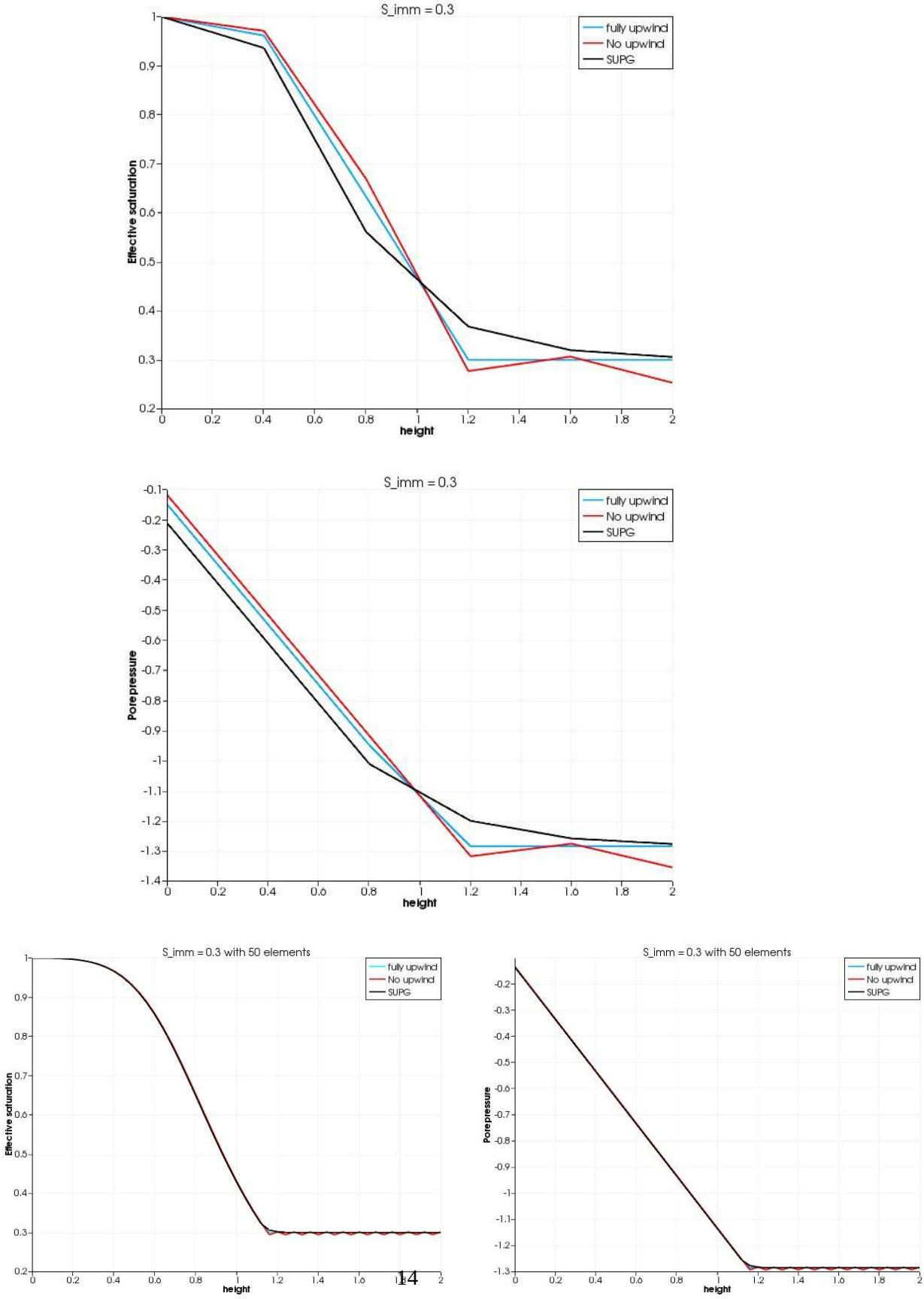

Figure 5.1: Results for $S_{\text{imm}} = 0.3$. Gravity points to the left. Top picture: Effective saturation. Middle picture: Pore pressure. Bottom pictures: The situation with 50 elements in the x direction instead of just 5. In each picture the blue line is with full upwinding, the black line with SUPG, and the red line is without upwinding where oscillatory results can be observed in addition to $S_{\text{eff}} < S_{\text{imm}}$.

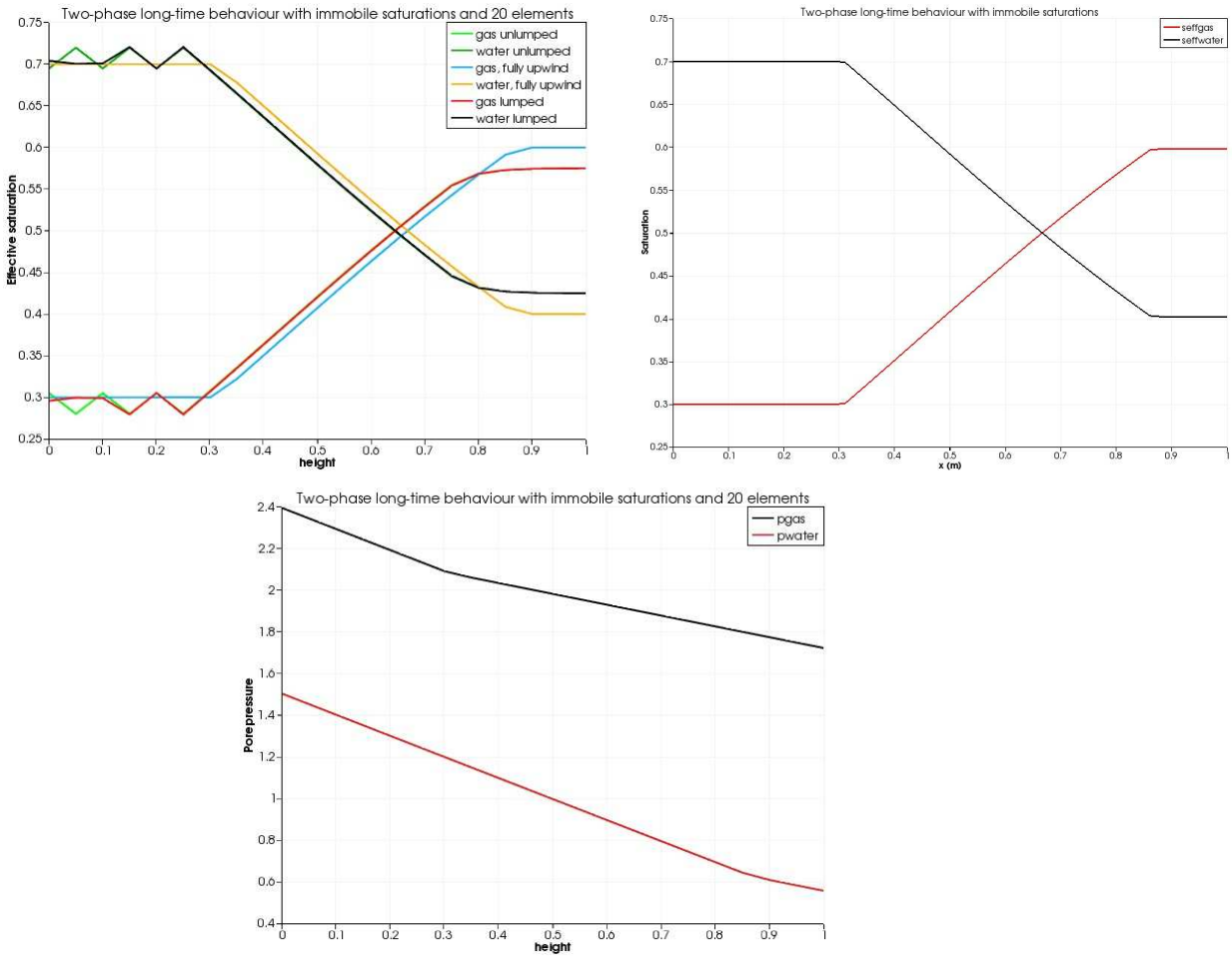

Figure 5.2: Two-phase long-time results for $S_{\text{imm}}^{\text{gas}} = 0.3$ and $S_{\text{imm}}^{\text{water}} = 0.4$. Left: 20-element simulation without time-derivative lumping and with SUPG with $P_{\text{SUPG}} = 0.1$ for water and $P_{\text{SUPG}} = 0.01$ for gas; with lumping and the same SUPG parameters; and without mass lumping but with full upwinding. Right: 200-element simulation. Bottom: the porepressures, demonstrating that each porepressure follows Eqn (5.2) unless it is at immobile saturation in which case it is forced to follow the porepressure of the other phase.

6 Piecewise linear and half-Gaussian sinks

The MOOSE implementation allows users to specify sinks and sources acting at boundaries that are functions of porepressure. This chapter tests that these sinks and sources act as specified. These tests are part of the automatic test suite that is run every time the code is updated.

A 2D model with $0 \le x \le 1$ and $0 \le y \le 1$ with just a single element is subjected to sink fluxes from its left and right boundaries. Because it is a single element no fluid flow within the element occurs. The following fluid properties are used:

Constant fluid bulk modulus	1 Pa
Fluid density at zero pressure	$1\,\mathrm{kg.m^{-3}}$
Residual fluid saturation	0.1
Residual air saturation	0.1
Van Genuchten m	0.5
Van Genuchten α	$1\,\mathrm{Pa^{-1}}$
Power-type relative permeabilty n	2
κ_{xx}	$10^{-5}\,\mathrm{m^2}$
Porosity	0.1

In the first set of two tests a piecewise-linear sink is applied with strength:

$$\text{sink flux } (\mathrm{kg.m^{-1}.s^{-1}}) = \begin{cases} 1 & \text{for } p \le 0 \\ 1+p & \text{for } 0 < p < 1 \\ 2 & \text{for } p \ge 1 \end{cases} \tag{6.1}$$

The first test uses no upwinding, while the second fully-upwinds the flux. The sink flux is recorded by into a Postprocessor by MOOSE. It is remotely possible that the MOOSE implementation *applies* the sink flux incorrectly, but *records* it as a Postprocessor correctly as specified by Eqn (6.1). Therefore the simulation also records the fluid mass and mass-balance error in order to check that the fluid mass is indeed being reduced correctly by the sink flux. The initial condition is $p = 2\,\mathrm{Pa}$, and the simulation is run for $0.2\,\mathrm{s}$ with 100 time steps. The expected behaviour is demonstrated in Figure 6.1.

In the second test a piecewise-linear sink is applied with strength:

$$\text{sink flux } (\mathrm{kg.m^{-1}.s^{-1}}) = \begin{cases} 2\exp(-0.5(P-1)^2) & \text{for } p < 1 \\ 2 & \text{for } p \ge 1 \end{cases} \tag{6.2}$$

This is called a half-Gaussian sink flux and may be used to model evapotranspiration. The sink flux is recorded by into a Postprocessor by MOOSE. It is remotely possible that the MOOSE implementation *applies* the sink flux incorrectly, but *records* it as a Postprocessor correctly as specified by Eqn (6.2). Therefore the simulation also records the fluid mass and mass-balance

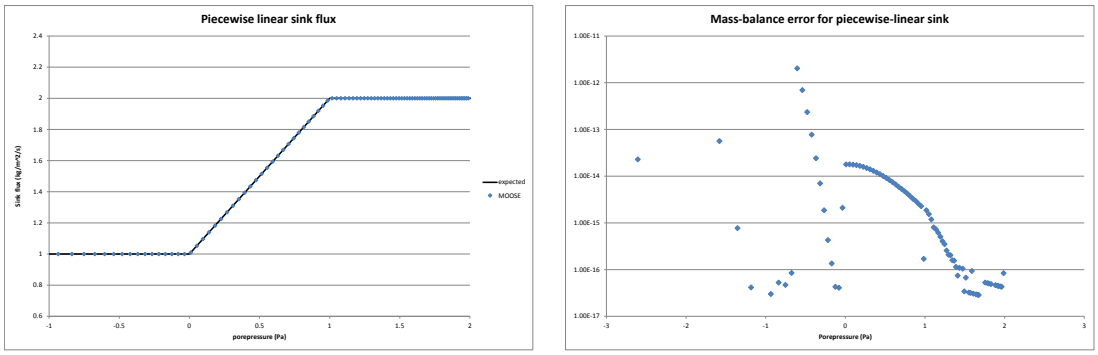

Figure 6.1: Left: Comparison between the MOOSE result (in dots), and the expected behaviour of the sink flux given by Eqn (6.1). Right: The mass-balance error is small for the simulation described demonstrating that the recorded sink flux is truly reducing the mass in the correct way.

error in order to check that the fluid mass is indeed being reduced correctly by the sink flux. The initial condition is $p = 2$ Pa, and the simulation is run for 0.4 s with 100 time steps. The expected behaviour is demonstrated in Figure 6.2.

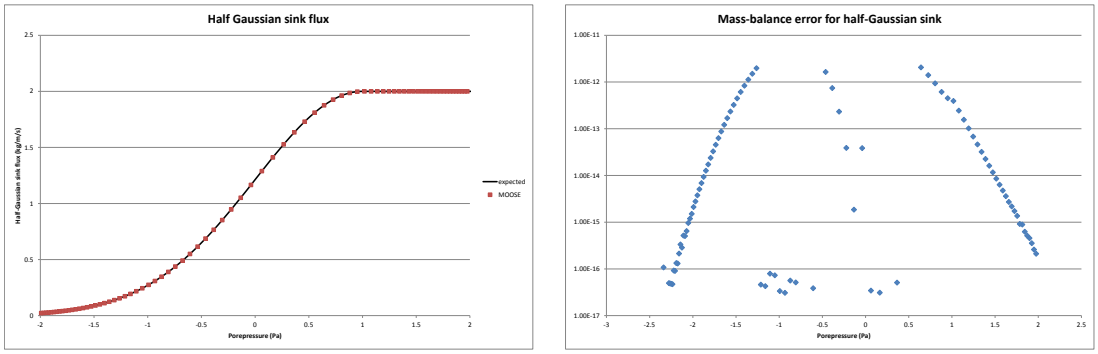

Figure 6.2: Left: Comparison between the MOOSE result (in dots), and the expected behaviour of the sink flux given by Eqn (6.2). Right: The mass-balance error is small for the simulation described demonstrating that the recorded sink flux is truly reducing the mass in the correct way.

In the third set of two tests a piecewise-linear sink with relative permeability and mobility affects is used. The flux strength is:

$$\text{sink flux (kg.m}^{-1}\text{.s}^{-1}) = \frac{\rho \kappa_{xx} \kappa_{\text{rel}}}{\mu} \times \begin{cases} 100 & \text{for } p \leq -1 \\ 150 + 50p & \text{for } -1 < p < 1 \\ 200 & \text{for } p \geq 1 \end{cases} \tag{6.3}$$

The first test uses no upwinding, while the second fully-upwinds the flux. The sink flux is recorded by into a Postprocessor by MOOSE. It is remotely possible that the MOOSE implementation *applies* the sink flux incorrectly, but *records* it as a Postprocessor correctly as specified by Eqn (6.3). Therefore the simulation also records the fluid mass and mass-balance error in order to check that the fluid mass is indeed being reduced correctly by the sink flux. The initial

condition is $p = 2\,\text{Pa}$, and the simulation is run for $0.2\,\text{s}$ with 100 time steps. The expected behaviour is demonstrated in Figure 6.3.

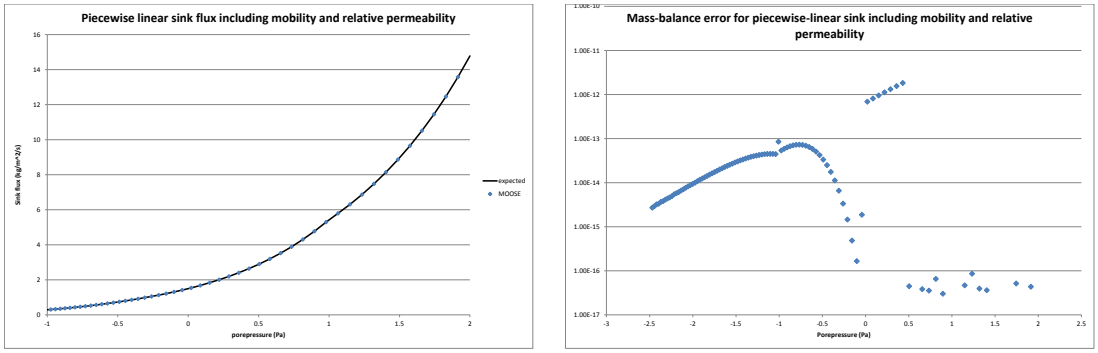

Figure 6.3: Left: Comparison between the MOOSE result (in dots), and the expected behaviour of the sink flux given by Eqn (6.3). Right: The mass-balance error is small for the simulation described demonstrating that the recorded sink flux is truly reducing the mass in the correct way.

7 PolyLine sink

The MOOSE implementation allows users to specify sinks and sources acting along polylines that are functions of porepressure. This is primarily designed to model stream sources/sinks. This chapter tests that these sinks and sources act as specified. The test is part of the automatic test suite that is run every time the code is updated.

A 3D model with $-1 \le x \le 1$, $-1 \le y \le 1$ and $-1 \le z \le 1$ with just a single element is subjected to polyline sink flux acting at its centre point. Because it is a single element with the polyline sitting at its centre, no fluid flow within the element occurs. The following fluid properties are used:

Constant fluid bulk modulus	2 GPa
Fluid density at zero pressure	1000 kg.m^{-3}

The test is fully-saturated, so the van Genuchten parameters, etc, are irrelevant. The initial porepressure is set to 10 MPa, and the polyline sink flux is applied with strength:

$$\text{sink flux (kg.s}^{-1}) = \begin{cases} 1 & \text{for } p \le 2\,\text{MPa} \\ 1+(p-2)/6 & \text{for } 2 < p < 8\,\text{MPa} \\ 2 & \text{for } p \ge 8\,\text{MPa} \end{cases} \tag{7.1}$$

The sink flux is recorded by into a Postprocessor by MOOSE. It is remotely possible that the MOOSE implementation *applies* the sink flux incorrectly, but *records* it as a Postprocessor correctly as specified by Eqn (7.1). Therefore the simulation also records the fluid mass and mass-balance error in order to check that the fluid mass is indeed being reduced correctly by the sink flux. The simulation is run for 2.5 s using 25 time steps.

The expected behaviour is demonstrated in Figure 7.1.

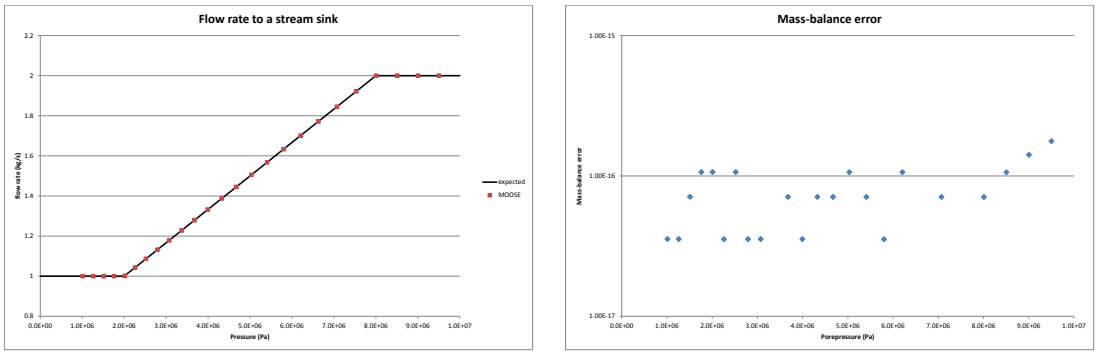

Figure 7.1: Left: Comparison between the MOOSE result (in dots), and the expected behaviour of the sink flux given by Eqn (7.1). Right: The mass-balance error is small for the simulation described demonstrating that the recorded sink flux is truly reducing the mass in the correct way.

8 A pressure pulse in the fully saturated situation

Richards' equation for flow through a fully saturated medium without gravity and without sources is just Darcy's equation

$$\frac{\partial}{\partial t}\phi\rho = \nabla_i \left(\frac{\rho\kappa_{ij}}{\mu}\nabla_j P \right) , \tag{8.1}$$

with notation described in the Theory Manual. Using $\rho \propto \exp(P/K)$, where K is the fluid bulk modulus, Darcy's equation becomes

$$\frac{\partial}{\partial t}\rho = \nabla_i \alpha_{ij} \nabla\rho , \tag{8.2}$$

with

$$\alpha_{ij} = \frac{\kappa_{ij}B}{\mu\phi} . \tag{8.3}$$

Here I've assumed the porosity and bulk modulus are constant in space and time.

Consider the one-dimensional case were the spatial dimension is the semi-infinite line $x \geq 0$. Suppose that initially the pressure is constant, so that

$$\rho(x, t = 0) = \rho_0 \quad \text{for} \quad x \geq 0 . \tag{8.4}$$

Then apply a fixed-pressure Dirichlet boundary condition at $x = 0$ so that

$$\rho(x = 0, t > 0) = \rho_\infty \tag{8.5}$$

The solution of the above differential equation is well known to be

$$\rho(x,t) = \rho_\infty + (\rho_0 - \rho_\infty)\,\mathrm{Erf}\left(\frac{x}{\sqrt{4\alpha t}} \right) , \tag{8.6}$$

where Erf is the error function.

This is verified by using the following twelve tests on a line of 10 elements.

1. Steady state 1-phase analysis to demonstrate that the steady-state of $\rho = \rho_\infty$ is achieved.
2. Transient 1-phase analysis with an unlumped time derivative.
3. Transient 1-phase analysis with a lumped time derivative.
4. Steady state 2-phase analysis with a fully-water saturated configuration.

5. Transient 2-phase analysis with unlumped time derivatives.

6. Transient 2-phase analysis with lumped time derivatives.

Each of these is run with SUPG, and with full upwinding. An example verification is shown in Figure 8.1. These tests run rapidly and are part of the automatic test suite.

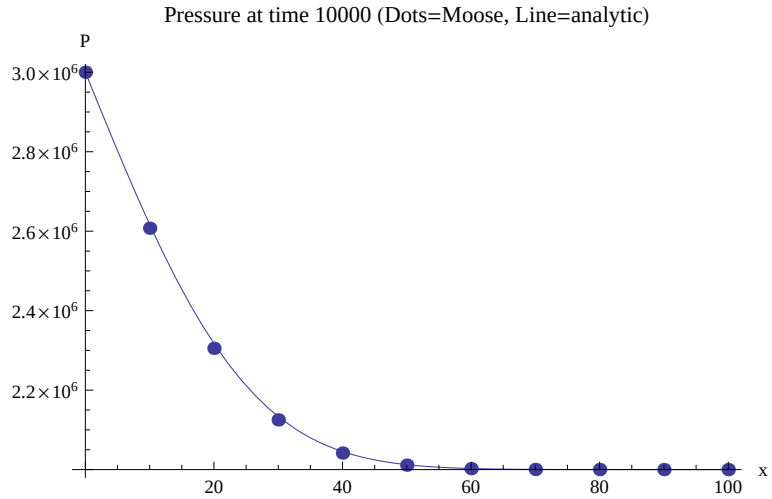

Figure 8.1: Comparison between the MOOSE result (in dots), and the exact analytic expression given by Eqn (8.6). This test had 10 elements in the x direction, with $0 \leq x \leq 100\,\mathrm{m}$, and ran for a total of 10^4 seconds with 10 timesteps. The parameters were $B = 2\,\mathrm{GPa}$, $\kappa_{xx} = 10^{-15}\,\mathrm{m}^2$, $\mu = 10^{-3}\,\mathrm{Pa.s}$, $\phi = 0.1$, with initial pressure $P = 2\,\mathrm{MPa}$, and applied pressure $P = 3\,\mathrm{MPa}$ at $x = 0$. For greater spatial resolution and smaller timesteps the agreement increases. Both the single-phase simulation and the 2-phase fully-water-saturated simulation give identical results for the water porepressure (regardless of upwinding scheme.

9 Newton cooling from a bar

This test demonstrates that MOOSE behaves correctly when a simulation contains a sink. The sink is a piecewise linear function of pressure.

Darcy's equation for flow through a fully saturated medium without gravity and without sources is

$$\frac{\partial}{\partial t}\phi\rho = \nabla_i\left(\frac{\rho\kappa_{ij}}{\mu}\nabla_j P\right) , \tag{9.1}$$

with notation described in the Theory Manual. Using $\rho \propto \exp(P/B)$, where B is the fluid bulk modulus, Darcy's equation becomes

$$\frac{\partial}{\partial t}\rho = \nabla_i\alpha_{ij}\nabla_j\rho , \tag{9.2}$$

with

$$\alpha_{ij} = \frac{\kappa_{ij}B}{\mu\phi} . \tag{9.3}$$

Here I've assumed the porosity and bulk modulus are constant in space and time.

Consider the one-dimensional case where a bar sits between $x = 0$ and $x = L$ with initial pressure distribution so $\rho(x,t=0) = \rho_0(x)$. Maintain the end $x = 0$ at constant pressure, so that $\rho(x=0,t) = \rho_0(0)$. At the end $x = L$, prescribe a sink flux

$$\left.\frac{\partial\rho}{\partial x}\right|_{x=L} = -C\left(\rho-\rho_e\right)_{x=L} , \tag{9.4}$$

where ρ_e is a fixed quantity ("e" stands for "external"), and C is a constant conductance. This corresponds to the flux

$$\left.\frac{\partial P}{\partial x}\right|_{x=L} = -CB\left(1-e^{(P_e-P)/B}\right)_{x=L} , \tag{9.5}$$

which can easily be coded into a MOOSE input file: the flux is $\rho\kappa\nabla P/\mu = -CB\kappa(e^{P/B} - e^{P_e/B})/\mu$, and this may be represented by a piecewise linear function of pressure.

The solution of this problem is well known and is

$$\rho(x,t) = \rho_0(0) - \frac{\rho_0(0)-\rho_e}{1+LC}Cx + \sum_{n=1}^{\infty} a_n \sin\frac{k_n x}{L} e^{-k_n^2\alpha t/L^2} , \tag{9.6}$$

where k_n is the n^{th} positive root of the equation $LC\tan k + k = 0$ (k_n is a little bigger than $(2n-1)\pi/2$), and a_n is determined from

$$a_n\int_0^L \sin^2\frac{k_n x}{L}\,\mathrm{d}x = \int_0^L\left(\rho_0(x)-\rho_0(0)+\frac{\rho_0(0)-\rho_e}{1+LC}Cx\right)\sin\frac{k_n x}{L}\,\mathrm{d}x , \tag{9.7}$$

which may be solved numerically (I have used Mathematica to generate the solution in Figure 9.1).
The problem is solved in MOOSE using the following parameters:

Bar length	100 m
Bar porosity	0.1
Bar permeability	10^{-15} m^2
Gravity	0
Water density	1000 kg.m^{-3}
Water viscosity	0.001 Pa.s
Water bulk modulus	1 MPa
Initial porepressure P_0	2 MPa
Environmental pressure P_e	0
Conductance C	0.05389 m^{-1}

This conductance is chosen so at steadystate $\rho(x = L) = 2000\,\mathrm{kg.m^{-3}}$.

The problem is solved using 1000 elements along the x direction ($L = 100$ m), and using 100 time-steps of size 10^6 s. Using fewer elements or fewer timesteps means the agreement with the theory is marginally poorer. Two tests are performed: one with a lumped time derivative and one with an unlumped derivative, giving almost indistinguishable results. The problem is also solved using the steadystate solver. In this case the initial condition is $P = 2 - x/L$ MPa, since the uniform $P = 2$ MPa does not converge. The results are shown in Figure 9.1.

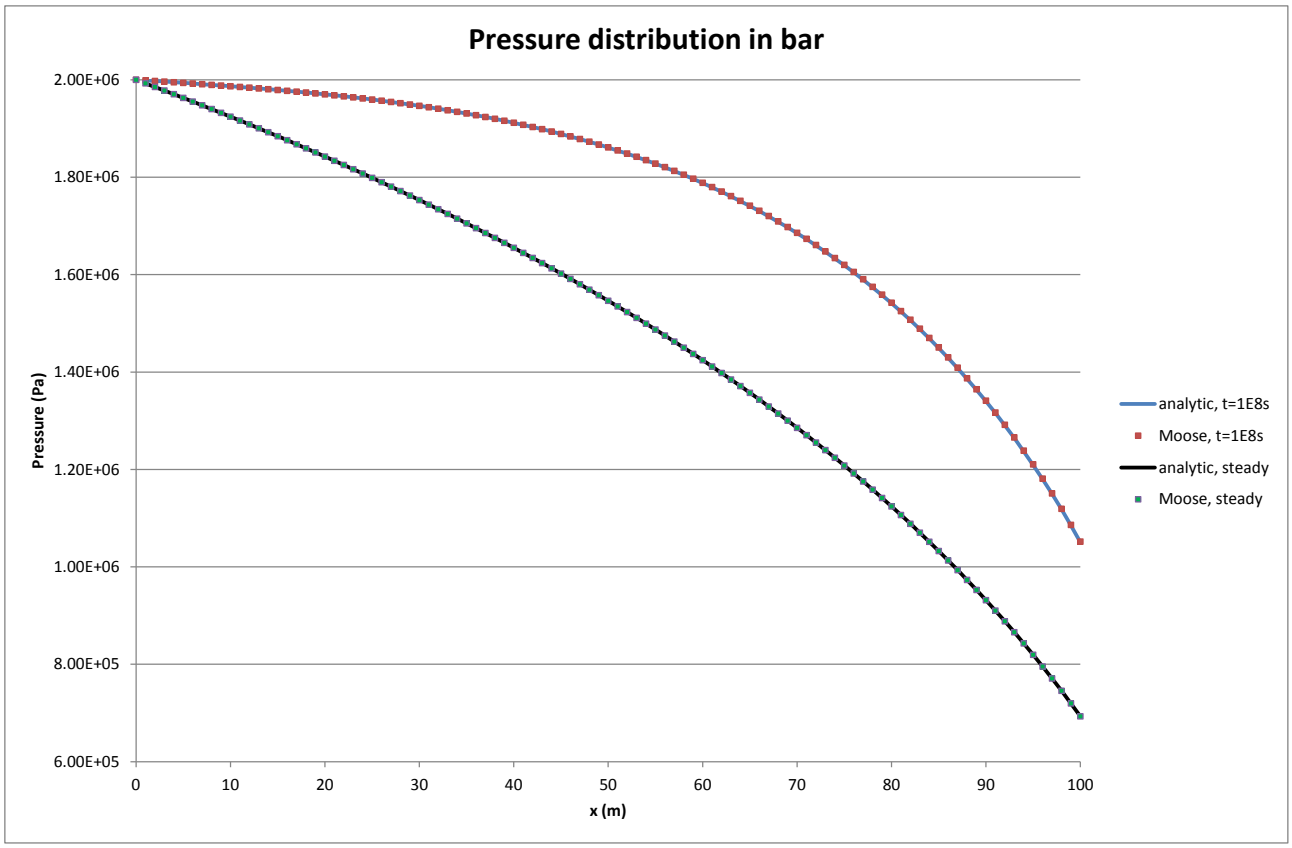

Figure 9.1: The porepressure in the bar at $t = 10^8$ s, and at steadystate. The pressure at $x = 0$ is held fixed, while the sink is applied at $x = 100$ m. MOOSE agrees well with theory demonstrating that piecewise-linear sinks/sources are correctly implemented in MOOSE.

10 The Theis problem

The Theis problem is related to an aquifer pumping test where water is withdrawn at a constant rate, Q ($m^3.s^{-1}$) from an isotropic, infinite, fully-saturated, confined aquifer. Water is withdrawn using a vertical borehole of negligible radius that spans the entire aquifer height, b (m). In the Theis solution, gravitational effects are ignored (the pressures at the bottom and top of the aquifer are is assumed equal). At some horizontal radial distance, r, from the borehole the pressure is measured. The geometry is shown in Figure 10.1.

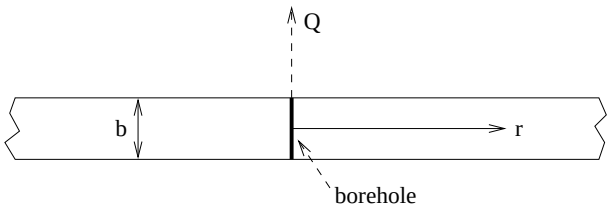

Figure 10.1: The Theis problem: An isotropic infinite, fully-saturated, confined aquifer of vertical height b is subjected to pumping at rate Q via a vertical borehole that spans the entire height of the aquifer. The pressure is measured at a radial distance r.

10.1 Derivation of the Theis solution

Theis solved this problem[1], and the derivation is given now using the Theory Manual notation. Darcy's equation reads

$$\phi \frac{\partial}{\partial t} \rho S = \nabla \cdot \left(\frac{\rho \kappa}{\mu} (\nabla P - \rho \mathbf{g}) \right) \ , \tag{10.1}$$

where ϕ is the aquifer porosity, t is time, ρ is the water density, S is the water saturation, ∇ is the spatial derivative, κ is the isotropic permeability, μ is the water viscosity, and P is the water pressure. Assume the following

- The problem is fully saturated, $S = 1$, and gravitational effects are ignored, $\mathbf{g} = \mathbf{0}$.
- The bulk modulus, $K_{\rm w}$, of water is constant so that $\rho = \rho_0 e^{P/K_{\rm w}}$.

[1] CV Theis, "The relation between the lowering of the piezometric surface and the rate and duration of discharge of a well using groundwater storage". Transactions, American Geophysical Union 16 (1935) 519–524

- The problem studied has the property

$$\left|\nabla^2 P\right| \gg \left|\frac{(\nabla P)^2}{K_{\rm w}}\right| . \tag{10.2}$$

  This inequality will be explored below.

Under these assumptions, Darcy's equation reads

$$\frac{\phi}{K_{\rm w}}\frac{\partial}{\partial t}P = \frac{K}{\mu}\nabla^2 P , \tag{10.3}$$

which, in this 2D case, has the standard exponential integral solution

$$P(r,t) = P_0 - \alpha\int_{\frac{r^2\phi\mu}{4t\kappa K_{\rm w}}}^{\infty}\frac{1}{u}e^{-u}\,{\rm d}u . \tag{10.4}$$

Applying the boundary condition at $r = 0$ that the rate of change of volume of water in the aquifer is Q yields the coefficient α, and the solution becomes

$$P(r,t) = P_0 - \frac{Q\mu}{4\pi b\kappa}\int_{\frac{r^2\phi\mu}{4t\kappa K_{\rm w}}}^{\infty}\frac{1}{u}e^{-u}\,{\rm d}u . \tag{10.5}$$

10.2 Transmissivity, Storativity and Well function

The hydrogeology literature uses different notation. It defines the head, $h = P/\rho g$; the transmissivity, $T = \kappa\rho g b/\mu$; the storativity, $S = b\rho g\phi/K_{\rm w}$; and the well function $W(x) = \int_x^\infty u^{-1}e^{-u}{\rm d}u$, so that the Theis solution, Eqn (10.5) becomes

$$h(r,t) = h_0 - \frac{Q}{4\pi T}W\left(\frac{r^2 S}{4Tt}\right) . \tag{10.6}$$

10.3 Comparison with MOOSE

A Moose model defined by a cylinder of radius 3 km with 1500 hexahedral elements is created. The plan mesh is shown in Figure 10.2. The well is situated at $r = 0$, and the pressure is measured at $r = 50$ m. The pumping is modelled using a PolyLineSink with constant rate.

The following parameters are used:

Aquifer porosity, ϕ	0.1
Aquifer permeability, κ	10^{-10} m^2
Water viscosity, μ	0.001 Pa.s
Water bulk modulus, $K_{\rm w}$	2 GPa
Gravity	0.0
Aquifer thickness, b	20 m
Pumping rate, Q	0.2 m^3.s^{-1}

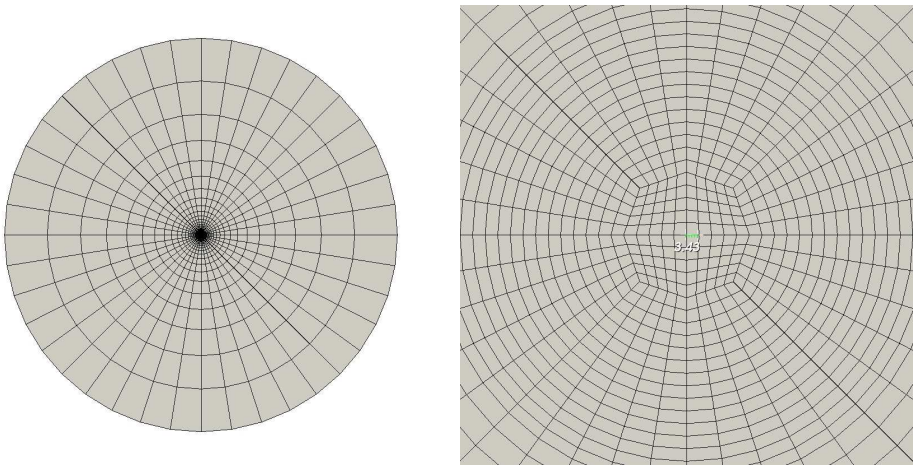

Figure 10.2: The mesh for the Theis problem has 1500 elements, and a radius of 3 km. Left: the whole plan mesh. Right: the region $r \leq 50$ m.

The van-Genuchten parameters, etc, are unimportant as this is a fully-saturated simulation.

Eqn (10.2) contains an important assumption of the Theis solution which constrains the validity of the result. Substituting the solution, Eqn (10.5), into the assumption yields

$$\frac{1}{u}e^{-u} \ll \frac{4\pi b\kappa K_{\rm w}}{Q\phi\mu} = \frac{4\pi bT}{QS} \ , \tag{10.7}$$

where

$$u = \frac{r^2\phi\mu}{4t\kappa K_{\rm w}} = \frac{r^2 S}{4tT} \ . \tag{10.8}$$

In the situation under study, substituting the numerical values given above yields $u^{-1}e^{-u} \ll 2.5\times 10^6$, or $u \gg 4\times 10^{-7}$. When $r = 50$ m, this yields $t \ll 8\times 10^5$ s.

Figure 10.3 shows good agreement between the Theis solution and the MOOSE implementation. Both 1-phase and fully-water-saturated 2-phase models give the same result, both with and without time-derivative lumping. These four tests are not part of the automatic test suite since they take around 20 seconds to complete. They are therefore marked as "heavy" and is not run every time the code is updated. However, four similar tests (both 1-phase and fully-water-saturated 2-phase, both with and without mass lumping) on a coarser mesh with only 272 elements, that also take larger timesteps, give similar drawdowns (to within 0.1 m), and are part of the automatic test suite.

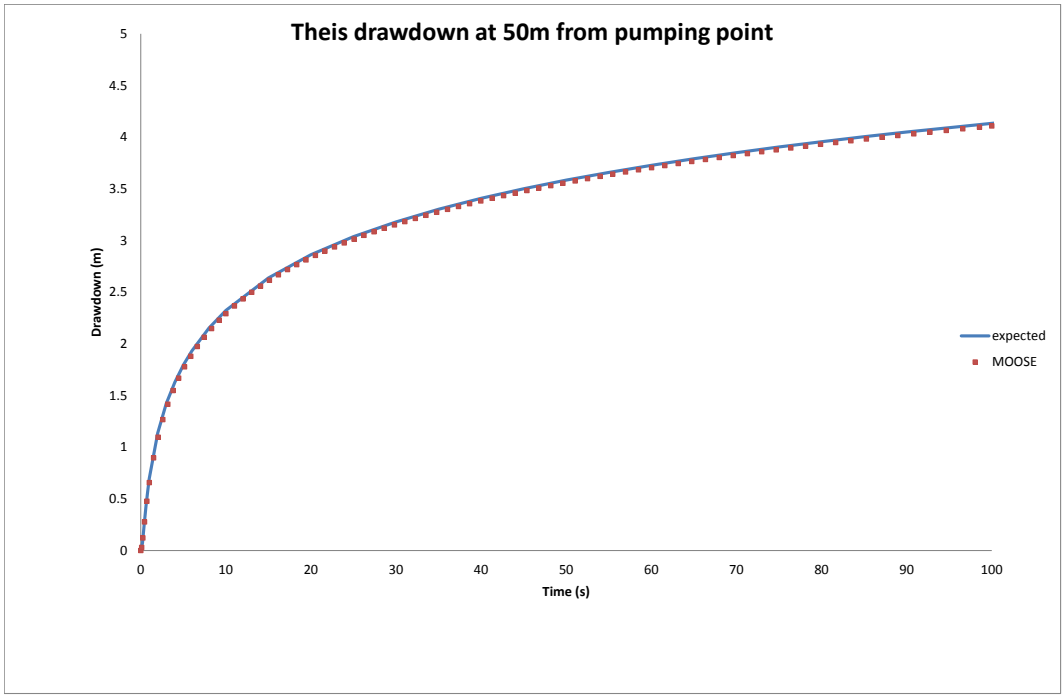

Figure 10.3: Comparison between the MOOSE result (in dots: both 1-phase and 2-phase fully-saturated, both with and without mass lumping give indistinguishable results and the expected behaviour of the drawdown as given by Eqn (10.5) (drawdown is $P/\rho g$, or $P/10000$ in this model).

11 Boreholes

As detailed in the Theory Manual, a borehole defined by a curve (or, most often, a straight line segment) in 3D space is modelled by a sequence of Dirac points. At each point, a flux is prescribed:

$$f = W|C(P - P_{\rm bh})|\frac{\rho\kappa_{\rm rel}}{\mu}(P - P_{\rm bh}) \ , \tag{11.1}$$

where P is the porepressure at the Dirac point, and $P_{\rm bh}$ is the borehole pressure at that point (an input parameter). The other parameters are: C, the character of the borehole (eg, "production" has $C = 1$ for $P > P_{\rm bh}$ and zero otherwise); ρ is the fluid density; $\kappa_{\rm rel}$ is the relative permeability; and μ is the fluid viscosity. The coefficient of proportionality, W, in this expression is a complicated function of the geometry of the finite element (or the neighbouring elements if the Dirac point is on an elemental boundary) and the rock permeability, and the borehole radius at that point.

11.1 Rotation matrices

The well constant W in Eqn (11.1) involves the rotation matrices that transforms between Cartesian (x,y,z) coordinates and coordinates in which the z axis lies along the local direction of the borehole.

- The first borehole test checks that these rotation matrices are formed correctly for random alignments of boreholes.

This test is very fast to run (it does not involve any fluid flow) and is part of the automatic test suite.

11.2 Fluxes

The automatic test suite also contains eight tests that check that Eqn (11.1) is correctly implemented for given W (the Peaceman formulation is used) by placing a vertical borehole through the centre of a single element, and measuring the fluid flow to the borehole as a function of porepressure P. These eight tests are:

- A production borehole with $P_{\rm bh} = 0$, with a fully-saturated medium, and with no upwinding or full upwinding of the borehole flux
- An injection borehole with $P_{\rm bh} = 10\,{\rm MPa}$, with a fully-saturated medium, and with no upwinding or full upwinding of the borehole flux

- A production borehole with $P_{\rm bh} = -1\,{\rm MPa}$, with an unsaturated medium, and with no upwinding or full upwinding of the borehole flux
- An injection borehole with $P_{\rm bh} = 0$, with an unsaturated medium, and with no upwinding or full upwinding of the borehole flux

The parameters common to these tests are:

Element size	$2 \times 2 \times 2\,{\rm m}^3$
Borehole radius	$0.1\,{\rm m}$
Bar permeability	$10^{-12}\,{\rm m}^2$
Gravity	0
Unit fluid weight	0
Fluid reference density	$1000\,{\rm kg.m}^{-3}$
Fluid bulk modulus	$2\,{\rm GPa}$
Fluid viscosity	$10^{-3}\,{\rm Pa.s}$
Van Genuchten α	$10^{-5}\,{\rm Pa}$
Van Genuchten m	0.8
Immobile saturation	0
Relative permeability n	2

It is remotely possible that the MOOSE implementation *applies* the borehole flux incorrectly, but *records* it as a Postprocessor correct as specified by Eqn (11.1). Therefore, these four simulations also record the fluid mass and mass-balance error in order to check that the fluid mass is indeed being correctly changed by the borehole. Figure 11.1 demonstrates that Eqn (11.1) is indeed correctly implemented in MOOSE.

11.3 Comparison with analytic solution

The Richards' equation for a fully-saturated medium with $\rho \propto \exp(P/B)$ and constant bulk modulus B becomes Darcy's equation

$$\frac{\partial}{\partial t}\rho\nabla_i\alpha_{ij}\nabla_j\rho \tag{11.2}$$

where $\alpha_{ij} = \kappa_{ij}B/(\mu\phi)$, with notation described in the Theory Manual. In the isotropic case (where $\kappa_{ij} = \kappa\delta_{ij}$), the steadystate equation is just Laplace's equation

$$\nabla^2\rho = 0\,, \tag{11.3}$$

Place a borehole of radius $r_{\rm bh}$ and infinite length oriented along the z axis. Then the situation becomes 2D and can be solved in cylindrical coordinates, with $\rho = \rho(r,\theta)$ and independent of z. If the pressure at the borehole wall $r = r_{\rm bh}$ is $P_{\rm bh}$, then the fluid density is $\rho_{\rm bh} \propto \exp(P_{\rm bh}/B)$. Assume that at $r = R$ the fluid pressure is held fixed at P_R, or equivalently the density is held fixed at ρ_R. Then the solution of Laplace's equation is well-known to be

$$\rho = \rho_{\rm bh} + (\rho_R - \rho_{\rm bh})\frac{\log(r/r_{\rm bh})}{\log(R/r_{\rm bh})}\,. \tag{11.4}$$

This is the fundamental solution used by Peaceman and others to derive expressions for W by comparing with numerical expressions resulting from Eqn (11.1) (see Theory Manual for more details).

Chen and Zhang (see Theory manual) have derived an expression for W in the case where this borehole is placed at a node in a square mesh. The following three tests are part of the automatic test suite:

- The steadystate solution with a single borehole with W defined by Chen and Zhang's formula is compared with Eqn (11.4) to illustrate that the MOOSE implementation of a borehole is correct.
- The same test using a lumped time derivative.
- The same test using full upwinding from the nodes to the borehole.

Figure 11.3 shows this comparison. Most parameters in this study are identical to those given in the above table with the following exceptions: the mesh is shown in Fig 11.2; the permeability is $10^{-11}\,\mathrm{m}^2$; the borehole radius is $1\,\mathrm{m}$; the borehole pressure is $P_{\mathrm{bh}} = 0$; the outer radius is $r = 300\,\mathrm{m}$; and the outer pressure is $P_R = 10\,\mathrm{MPa}$.

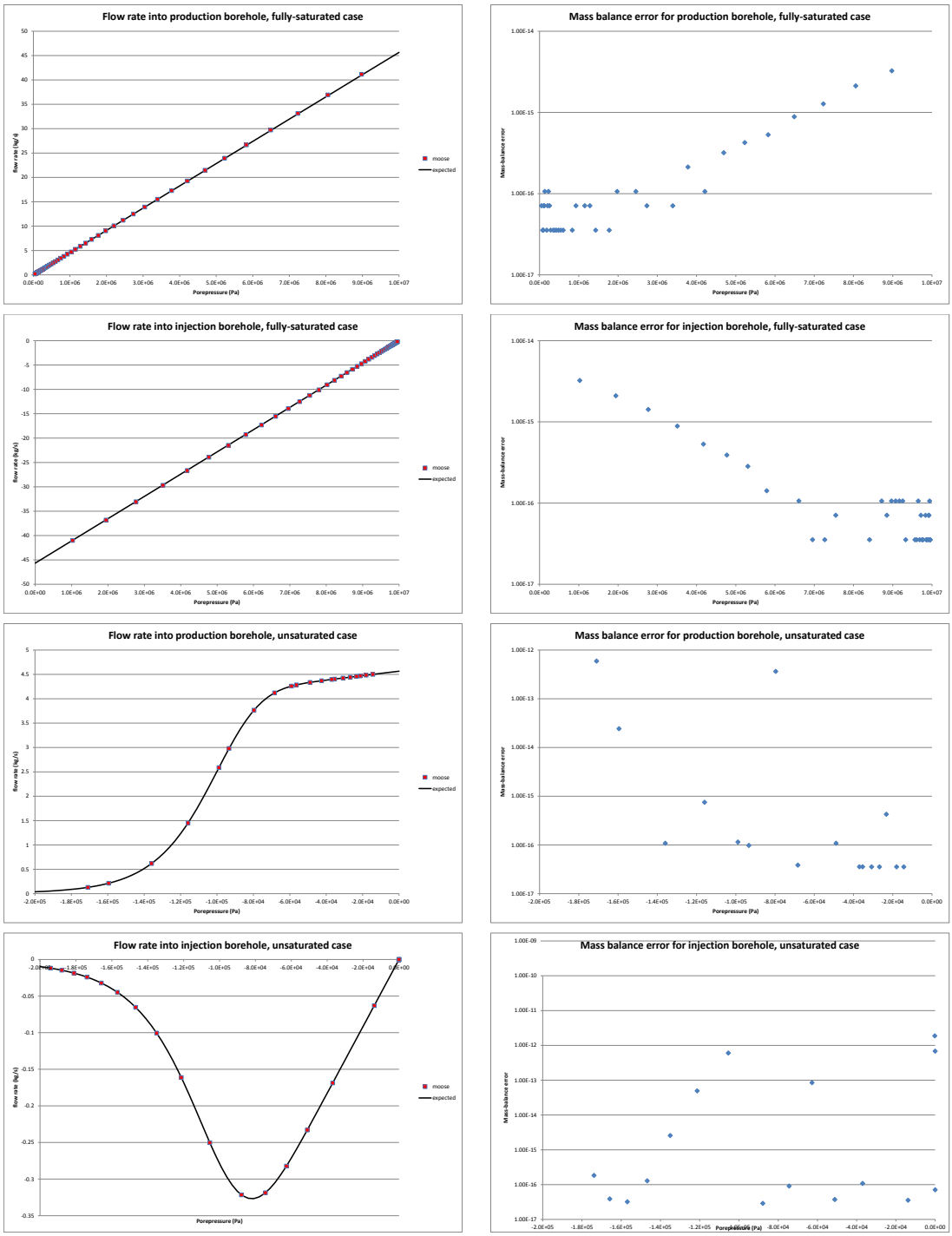

Figure 11.1: Left figures: Comparison between the MOOSE result (in dots), and the expected behaviour of the borehole flux given by Eqn (11.1) (as a line) for the cases listed in the text. Upwinding the mass flux from the nodes to the borehole makes no difference to these plots. Right figures: The mass balances, which are all small.

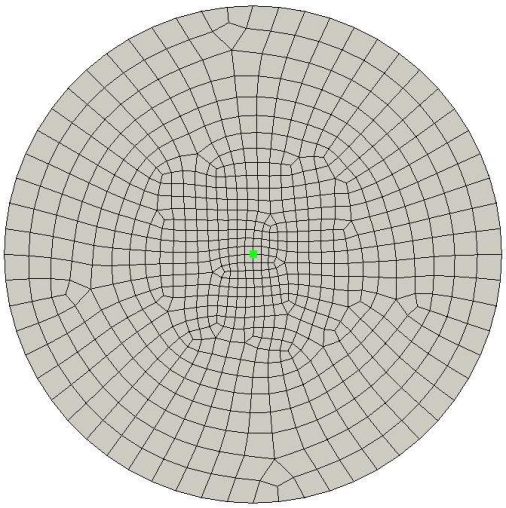

Figure 11.2: The mesh used in the comparison with Eqn (11.4), with the green dot indicating the position of the borehole. The central elements are $10 \times 10\,\mathrm{m}^2$, and the outer boundary is at $r = 300\,\mathrm{m}$.

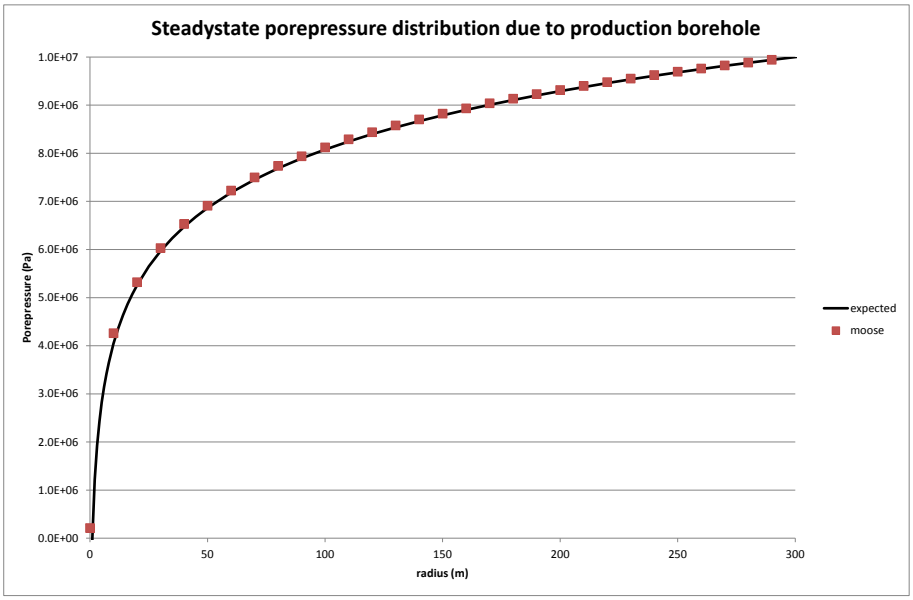

Figure 11.3: Comparison of the MOOSE results (dots) with the analytical solution Eqn (11.4) for the steadystate porepressure distribution surrounding single borehole.

12 The analytic infiltration solution

The Richards' equation for an incompressible fluid reads in one spatial dimension (z) reads

$$\dot{S} = \nabla\left(D\nabla S\right) - \nabla K \ , \tag{12.1}$$

where

$$D(S) = -\frac{\kappa\kappa_{rel}}{\mu\phi}P_{\rm c}' \ , \tag{12.2}$$

$$K(S) = \frac{\rho g\kappa\kappa_{\rm rel}}{\mu\phi} \ . \tag{12.3}$$

Here $P_{\rm c} = -P$ which is the capillary pressure, and recall that $P_{\rm c}'(S) < 0$.

The analytic solution of this nonlinear diffusion-advection relevant to constant infiltration to groundwater has been derived Broadbridge and White[1] for certain functions D and K. The setup is shown in "Experiment 1" of Figure 14.1 (ignore the specified infiltration rate, initial saturation and height of sample). Broadbridge and White assume the hydraulic conductivity is

$$K(S) = K_n + (K_s - K_n)\frac{\Theta^2(C-1)}{C-\Theta} \ , \tag{12.4}$$

where

$$\Theta = \frac{S - S_n}{S_s - S_s} \ , \tag{12.5}$$

and the parameters obey $0 \le K_n < K_s$, $0 \le S_n \le S \le S_s \le 1$, and $C > 1$. The diffusivity is of the form $a(b-S)^{-2}$. This leads to very complicated relationships between the capillary pressure, P_c, and the saturation, except in the case where K_n is small, when they are related through

$$\frac{P_{\rm c}}{\lambda_s} = \frac{1-\Theta}{\Theta} - \frac{1}{C}\log\left(\frac{C-\Theta}{(C-1)\Theta}\right) \ , \tag{12.6}$$

with $\lambda_s > 0$ being the final parameter.

Broadbridge and White derive time-dependent solutions for constant recharge to one end of a semi-infinite line. This represents constant rainfall recharge to an initially unsaturated soil block, for instance. Their solutions are quite lengthy, so I will not write them here. To compare with MOOSE, I use the following parameters — the hydraulic parameters are those used in Figure 3 of Broadbridge and White:

[1] P Broadbridge, I White "Constant rate rainfall infiltration: A versatile nonlinear model, 1 Analytical solution". Water Resources Research 24 (1988) 145–154.

Bar length	20 m
Bar porosity	0.25
Bar permeability	1
Gravity	$0.1\,\mathrm{m.s^{-2}}$
Fluid density	$10\,\mathrm{kg.m^{-3}}$
Fluid viscosity	4 Pa.s
S_n	$0\,\mathrm{m.s^{-1}}$
S_s	$1\,\mathrm{m.s^{-1}}$
K_n	$0\,\mathrm{m.s^{-1}}$
K_s	$1\,\mathrm{m.s^{-1}}$
C	1.5
λ_s	2 Pa
Recharge rate R_*	0.5

Broadbridge and white consider the case where the initial condition is $S = S_s$, but this yields $P = -\infty$, which is impossible to use in a MOOSE model. Therefore the initial condition $P = -900\,\mathrm{Pa}$ is used which avoids any underflow problems. The recharge rate of $R_* = 0.5$ corresponds in the MOOSE model to a recharge rate of $0.5\rho\phi(\kappa_s - \kappa_n) = 1.25\,\mathrm{kg.m^{-2}.s^{-1}}$. Note that I've chosen $\frac{\rho g \kappa}{\mu\phi} = 1\,\mathrm{m.s^{-1}}$, so that the K_n and K_s may be encoded as $\kappa_n = 0$ and $\kappa_s = 1$ in the relative permeability function Eqn (2.4) in a straightforward way.

Figure 12.1 shows good agreement between the analytic solution of Broadbridge and White and the MOOSE implementation. There are minor discrepancies for small values of saturation: these get smaller as the temporal and spatial resolution is increased, but never totally disappear due to the initial condition of $P = -900\,\mathrm{Pa}$.

Two tests (with and without mass lumping) are part of the automatic test suite that is run every time the code is updated.

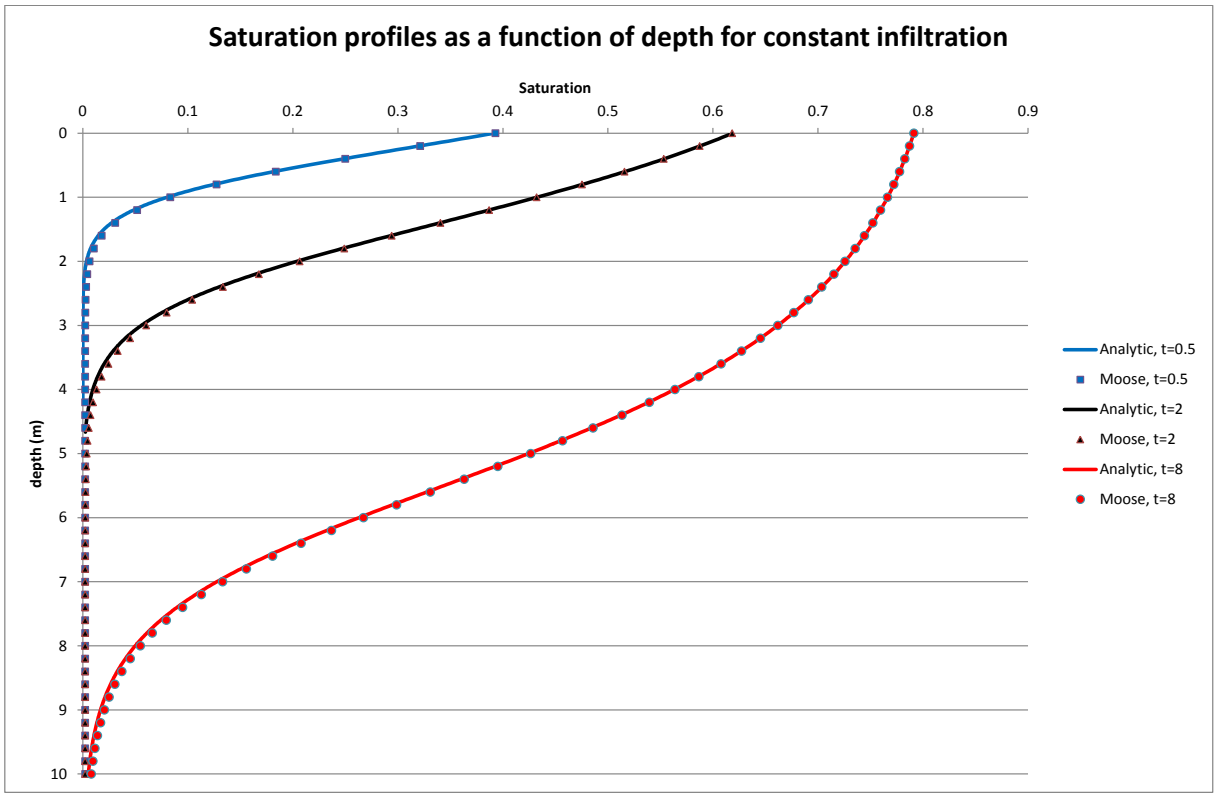

Figure 12.1: Comparison of the Broadbridge and White analytical solution with the MOOSE solution for 3 times. This figure is shown in the standard format used in the Broadbridge-White paper: the constant recharge is applied to the depth = 0 surface, and gravity acts downwards in this figure.

13 The analytic drainage solution

Warrick, Lomen and Islas[1] extended the analysis of Broadbridge and White (Chapter 12) to include the case of drainage from a medium. The setup is in "Experiment 2" of Figure 14.1. To obtain their analytical solutions, Warrick, Lomen and Islas make the same assumptions as Broadbridge and White concerning the diffusivity and conductivity of the medium. Their solutions are quite lengthy, so I will not write them here.

A MOOSE model with the parameters almost identical to those listed in Chapter 12 is compared with the analytical solutions. The only differences are that the "bar" length is 10000 m (to avoid any interference from the lower Dirichlet boundary condition), and $R_* = 0$ since there is no recharge. The initial condition is $P = 10^{-4}$ Pa: the choice $P = 0$ leads to poor convergence since by construction the Broadbridge-White capillary function is only designed to simulate the unsaturated zone $P < 0$ and a sensible extension to $P \geq 0$ is discontinuous at $P = 0$.

Figure 13.1 shows good agreement between the analytic solution and the MOOSE implementation. Any minor discrepancies get smaller as the temporal and spatial resolution increase.

This test is part of the automatic test suite that is run every time the code is updated.

[1] AW Warrick, DO Lomen and A Islas, "An analytical solution to Richards' Equation for a Draining Soil Profile", Water Resources Research 26 (1990) 253–258.

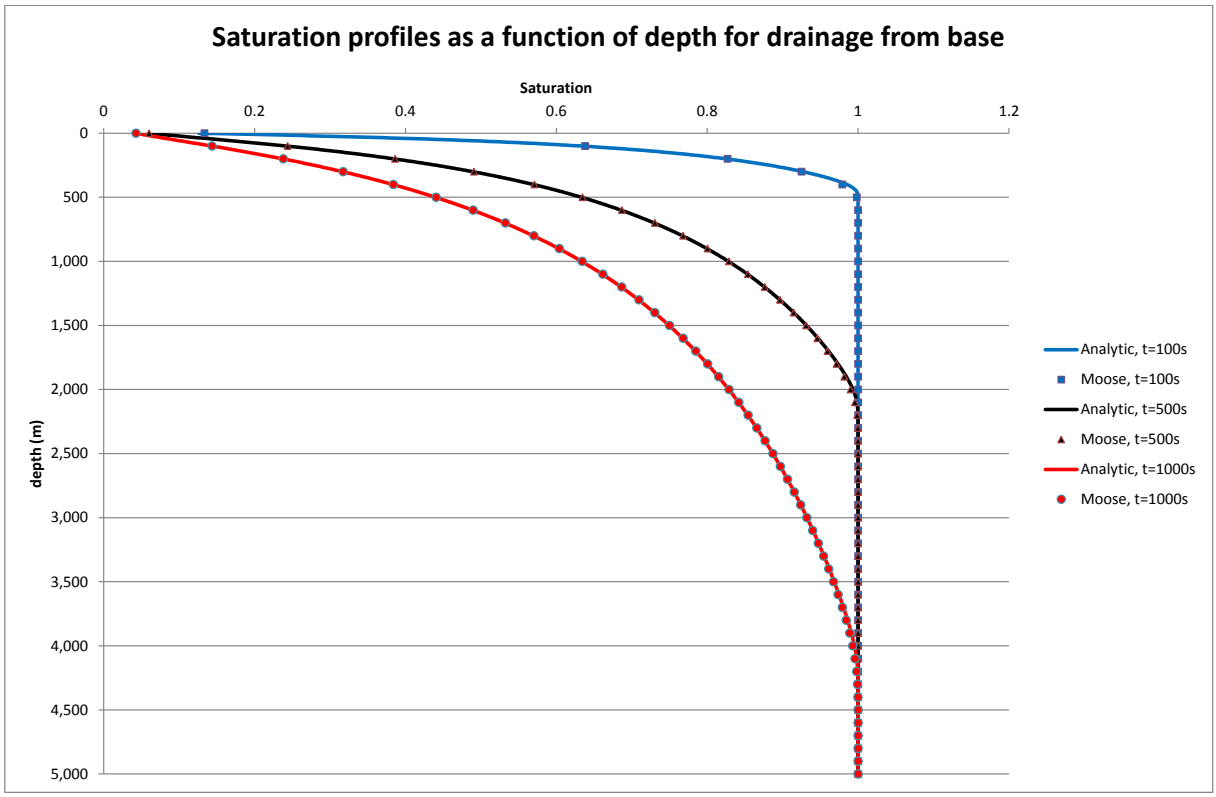

Figure 13.1: Comparison of the Warrick, Lomen and Islas analytical solution with the MOOSE solution for 3 times. This figure is shown in the standard format used in the literature: the top of the model is depth = 0 surface, and gravity acts downwards in this figure, with fluid draining from depth = ∞.

14 Infiltration and drainage

Forsyth, Wu and Pruess[1] describe a HYDRUS simulation of an experiment involving infiltration (experiment 1) and subsequent drainage (experiment 2) in a large caisson. The simulation is effectively one dimensional, and is shown in Figure 14.1.

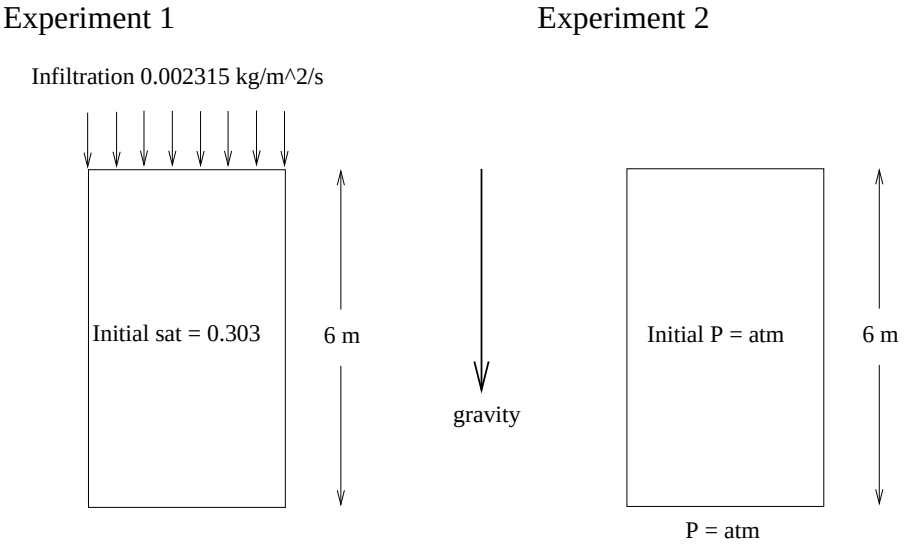

Figure 14.1: Two experimental setups from Forsyth, Wu and Pruess. Experiment 1 involves infiltration of water into an initially unsaturated caisson. Experiment 2 involves drainage of water from an initially saturated caisson.

The properties common to each experiment are:

[1] PA Forsyth, YS Wu and K Pruess, "Robust numerical methods for saturated-unsaturated flow with dry initial conditions in heterogeneous media", Advances in Water Resources 18 (1995) 25–38

Caisson	0.33
Caisson permeability	$2.95 \times 10^{-13}\,\mathrm{m}^2$
Gravity	$10\,\mathrm{m.s}^{-2}$
Water density	$1000\,\mathrm{kg.m}^{-3}$
Water viscosity	0.00101 Pa.s
Water bulk modulus	20 MPa
Water immobile saturation	0.0
Water residual saturation	0.0
Air residual saturation	0.0
Air pressure	0.0
van Genuchten α	$1.43 \times 10^{-4}\,\mathrm{Pa}^{-1}$
van Genuchten a	0.336
van Genuchten_1 cutoff	0.99

In each experiment 120 finite elements were used along the length of the Caisson. The modified van-Genuchten relative permeability curve was employed in order to improve convergence significantly. Hydrus also uses a modified van-Genuchten curve, although I couldn't find any details on the modification.

In experiment 1, the caisson is initially at saturation 0.303 ($P = -72620.4\,\mathrm{Pa}$), and water is pumped into the top with a rate $0.002315\,\mathrm{kg.m}^{-2}.\mathrm{s}^{-1}$. This causes a front of water to advance down the caisson. Figure 14.2 shows the agreement between MOOSE and the published result (this result was obtained by extracting data by hand from online graphics).

In experiment 2, the caisson is initially fully saturated at $P = 0$, and the bottom is held at $P = 0$ to cause water to drain via the action of gravity. Figure 14.2 shows the agreement between MOOSE and the published result.

Experiment 1 and the first 4 simulation days of experiment 2 are marked as "heavy" in the Richards' test suite since the simulations take around 3 seconds to complete. This means they are not run by default every time the code is updated, and must be run manually. However, the final 96 days of experiment 2 run quickly and are part of the automatic test suite.

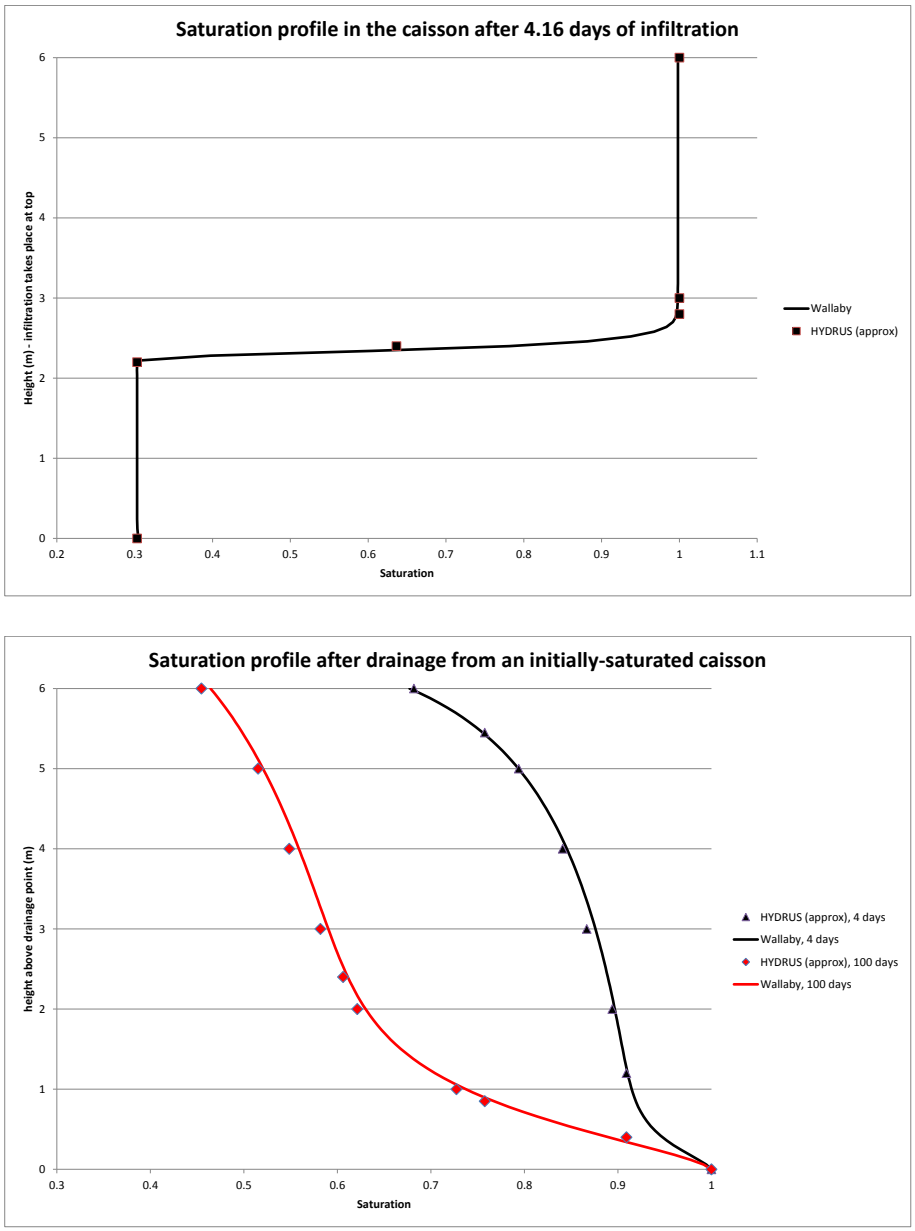

Figure 14.2: Saturation profiles in the caisson. Top: After 4.16 days of infiltration. Bottom: After drainage from an initially-saturated simulation (4 days and 100 days profiles). Note that the HYDRUS results are only approximate as I extrated the data by hand from online graphics.

15 The single-phase Buckley-Leverett problem

MOOSE is compared with a simple single-phase one-dimensional Buckley-Leverett problem[1]. The single-phase fluid moves in a region $0 \leq x \leq 15\,\mathrm{m}$. A fully-saturated front initially sits at position $x = 5$, while the region $x > 5$ is initially unsaturated. With zero suction function $P_c = 0$, there is no diffusion of the sharp front, and it progresses towards the right. This is a difficult problem to simulate numerically as maintaining the sharp front is hard. The front's speed is independent of the relative permeability, since the fluid is flowing from a fully-saturated region (where $\kappa_{\mathrm{rel}} = 1$). This problem is therefore a good test of the upwinding.

In the simulation below, the pressure at the left boundary is kept fixed at $P_0 = 0.98\,\mathrm{MPa}$, while the right boundary is kept fixed at $P_{15} = -20000\,\mathrm{Pa}$, so the difference is 1 MPa. The medium's permeability is set to $\kappa = 10^{-10}\,\mathrm{m}^2$ and its porosity is $\phi = 0.15$. It is not possible to use a zero suction function in the MOOSE implementation, but using the van Genuchten parameters $\alpha = 10^{-3}\,\mathrm{Pa}^{-1}$ and $m = 0.8$ approximates it. The fluid viscosity is $\mu = 10^{-3}\,\mathrm{Pa.s}$.

The initial condition is

$$P(t=0) = \begin{cases} P_0 - (P_0 - P_{15})x/5 & \text{for } x < 5 \\ P_{15} & \text{for } x \geq 5 \end{cases} , \tag{15.1}$$

which is shown in Figure 15.1. With the suction function defined above this gives

$$S(t=0) = \begin{cases} 1 & \text{for } x \leq 4.9 \\ 0.061 & \text{for } x \geq 5 \end{cases} \tag{15.2}$$

Good approximations for the pressure $P(x,t)$ and the front position $f(t)$ may be determined from

$$\begin{aligned} \frac{\mathrm{d}f}{\mathrm{d}t} &= -\frac{\kappa}{\phi\mu}\left.\frac{\partial P}{\partial x}\right|_{x=f} , \\ P(x,t) &= \begin{cases} P_0 - (P_0 - P_{15})x/f & \text{for } x \leq f \\ P_{15} & \text{for } x > f \end{cases} , \end{aligned} \tag{15.3}$$

which has solution

$$f(t) = \sqrt{f(0)^2 + \frac{2\kappa}{\phi\mu}(P_0 - P_{15})t} . \tag{15.4}$$

For the parameters listed above, the front will be at position $f = 9.6\,\mathrm{m}$ at $t = 50\,\mathrm{s}$. This solution is only valid for zero capillary suction. A nonzero suction function will tend to diffuse the sharp front.

[1] SE Buckley and MC Leverett (1942) "Mechanism of fluid displacements in sands". Transactions of the AIME **146** 107–116

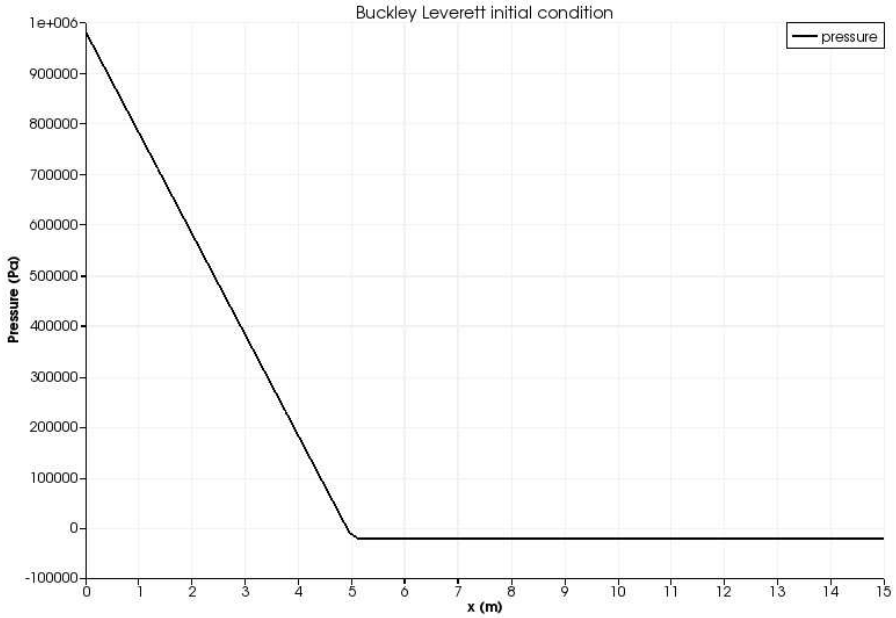

Figure 15.1: Initial setup of the Buckley-Leverett problem where porepressure is a piecewise linear function. The region $x \leq 4.9$ is fully saturated, while the region $x > 5$ has saturation 0.061. During simulation the value $P(x = 0) = 0.98 \times 10^6$ MPa is held fixed.

With coarse meshes it is impossible to simulate a sharp front, of course, since the front is spread over at least one element. It can be therefore quite advantageous to use mesh adaptivity in this test, since the mesh can be fine around the front where all the interesting dynamics occurs, and coarse elsewhere.

Figure 15.2 shows the results from a MOOSE simulation with a uniform mesh of size 0.1 m. At $t = 50$ s the front in this simulation sits at $x = 9.6$ m as desired. However, the simulation takes 3 minutes to complete due to the very low values of saturation obtained for van Genuchten $\alpha = 10^{-3}\,\mathrm{Pa}^{-1}$. Other simulations give similar results but run much faster. For instance, great speedups can be obtained by setting the van-Genuchten parameter $\alpha = 10^{-4}\,\mathrm{Pa}^{-1}$, but the front diffuses a little into the unsaturated region. Using an initial mesh of element size 1 m, and a minimum size of 0.125 m, with a maximum timestep of 0.3 s (to give the mesh time to adapt around the front),the front at $t = 50$ s sits between between $x = 9.9$ m and $x = 10.35$ m, and the simulation takes only 3 seconds. The automatic test suite contains three simulations (without mass lumping, with mass lumping, with mass lumping and full upwinding) with elements of size 0.1 m using a timestep of 2 s, which gives results very similar to these, and takes less than 2 seconds to run.

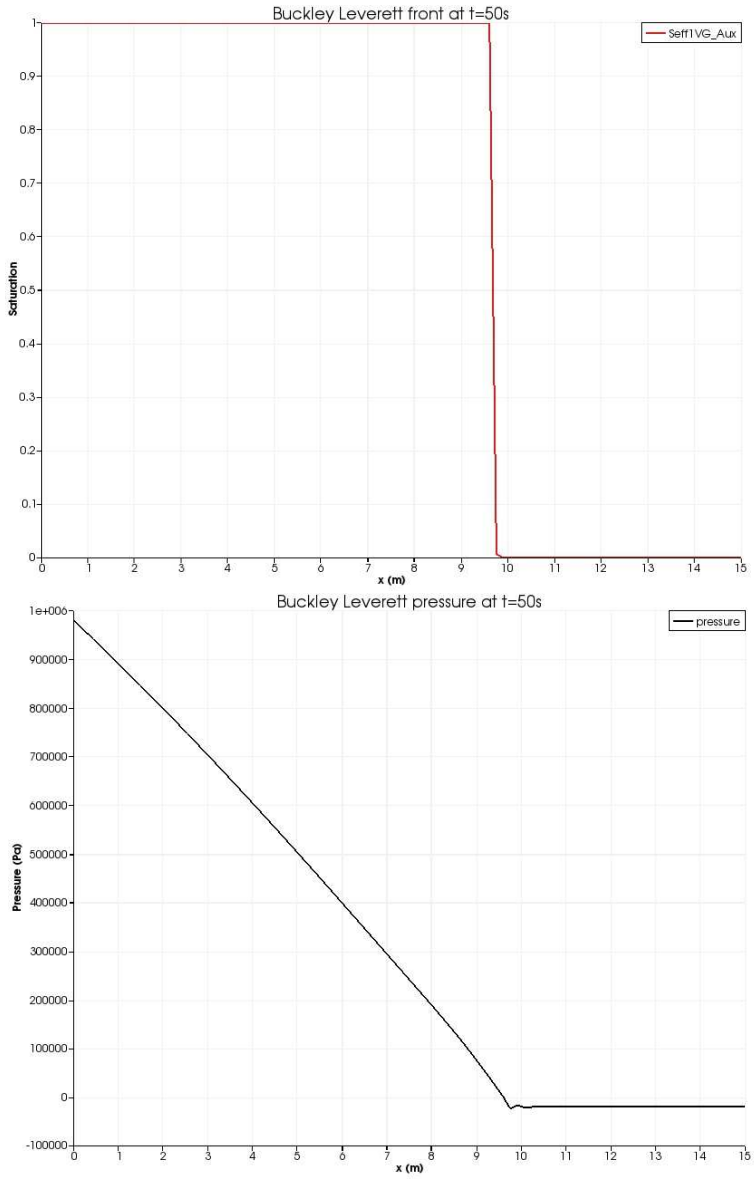

Figure 15.2: The MOOSE solution of the Buckley-Leverett problem at $t = 50\,\mathrm{s}$. Top: saturation. Bottom: porepressure. The front sits between $x = 9.6\,\mathrm{m}$ as expected from the analytical solution.

16 An excavation

"Excavations" are important in underground mining simulations. These are voids underground created by mining of material. On the boundary of the void the porepressure is fixed to a user-defined value, typically atmostpheric pressure. The size of the void changes with time as material is progressively mined. As discussed in the Theory Manual, these time-dependent boundary conditions are conveniently defined through a function. This section demonstrates that this procedure works as expected.

As depicted in Figure 16.1, a 3D simulation is run with region in the middle of the mesh that will be excavated. The simulation is run for 3×10^7 s which is the time taken to excavate the entire panel. Figure 16.2 shows the porepressure distribution at the plane of the panel at two times, and demonstrates that the correct boundary conditions are being applied.

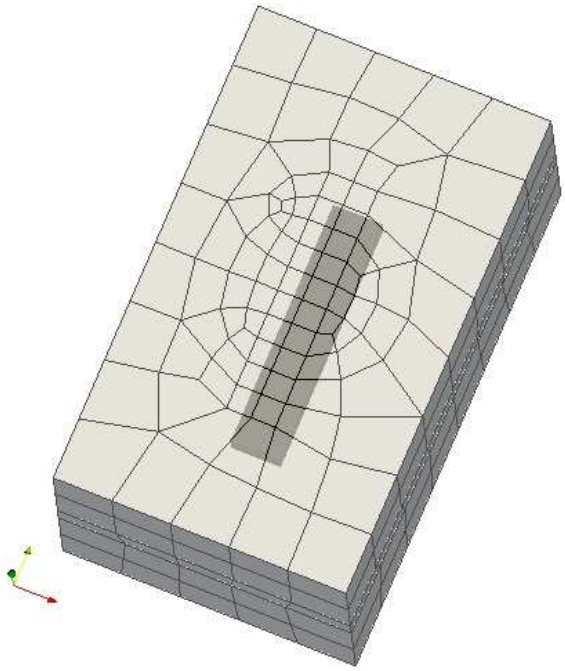

Figure 16.1: The 3D mesh used in the excavation test. This view is looking down on the mesh. In the middle of the solid there is a region that is excavated, and this is shown in a darker colour.

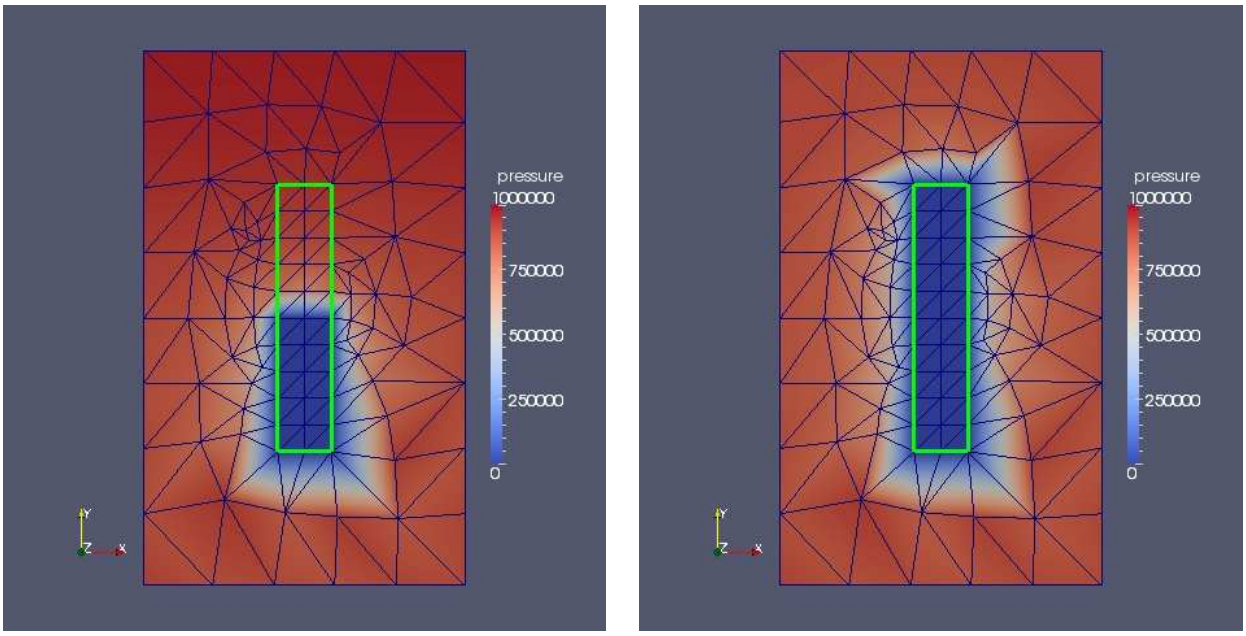

Figure 16.2: The porepressure contoured on a horizontal slice through the excavation region. The excavation region is shown as a green rectangle. The excavation is completed in 3×10^7 s and has $P = 0$ on the boundary. The left figure shows the porepressure at $t = 1.5 \times 10^7$ s, and the right figure shows $t = 3 \times 10^7$ s.

17 Water infiltration into a two-phase system

An analytic solution of the two-phase Richards' equations with gravity on a semi-infinite line $z \geq 0$, with a constant water infiltration flux at $z = 0$ has been derived by Rogers, Stallybrass and Clements [1]. The setup is very similar to the left-hand drawing in Figure 14.1, but ignore the initial saturation and infiltration rate, and the height of the sample is infinite. The authors assume incompressible fluids; linear relative permeability relationships; the "oil" (or "gas") viscosity is larger than the water viscosity; and, a certain functional form for the capillary pressure. When the oil viscosity is exactly twice the water viscosity, their effective saturation reads

$$S_{\text{eff}} = \frac{1}{\sqrt{1+\exp((P_c - A)/B)}} \ , \tag{17.1}$$

where $P_c = P_{\text{oil}} - P_{\text{water}}$ is the capillary pressure, and A and B are arbitrary parameters to be defined by the user in the MOOSE implementation. For other oil/water viscosity ratios $P_c = P_c(S_{\text{eff}})$ is more complicated, and note that their formulation allows $P_c < 0$, but only the particular form Eqn (17.1) need be used to validate the MOOSE implementation.

RSC's solutions are quite lengthy, so I will not write them here. To compare with MOOSE, the following parameters are used:

Bar length	10 m
Bar porosity	0.25
Bar permeability	10^{-5} m^2
Gravity[2]	0 m.s^{-2}
Water density	10 kg.m^{-3}
Water viscosity	10^{-3} Pa.s
Oil density	20 kg.m^{-3}
Oil viscosity	2×10^{-3} Pa.s
Capillary A	10 Pa
Capillary B	1 Pa
Initial water pressure	0 Pa
Initial oil pressure	15 Pa
Initial water saturation	0.08181
Initial oil saturation	0.91819
Water injection rate	1 kg s^{-1} m^{-2}

In the RSC theory water is injected into a semi-infinite domain, whereas of course the MOOSE implementation has finite extent ($0 \leq z \leq 10$ is chosen). Because of the near incompressibility

[1] C Rogers, MP Stallybrass and DL Clements "On two phase filtration under gravity and with boundary infiltration: application of a Backlund transformation" Nonlinear Analysis, Theory, Methods and Applications 7 (1983) 785–799

of the fluids (I choose the bulk modulus to be 2 GPa) this causes the porepressures to rise enormously, and the problem can suffer from precision-loss problems. Therefore, the porepressures are fixed at $z = 10$. This does not affect the progress of the water saturation front. Figure 17.1 shows good agreement between the analytic solution and the MOOSE implementation. Any minor discrepancies get smaller as the temporal and spatial resolution increase, as is suggested by the two comparisons in that figure.

The "low-resolution" tests (with SUPG or with full upwinding) which have 200 elements in $0 \leq z \leq 10$ and use 15 time steps, are part of the automatic test suite that is run every time the code is updated. Three "high-resolution" tests (without mass lumping and SUPG, with mass lumping and SUPG, with mass lumping and full upwinding) which have 600 elements, and use 190 time steps, are marked as "heavy" and so must be run manually. The mass lumping makes negligable difference to the result in this case.

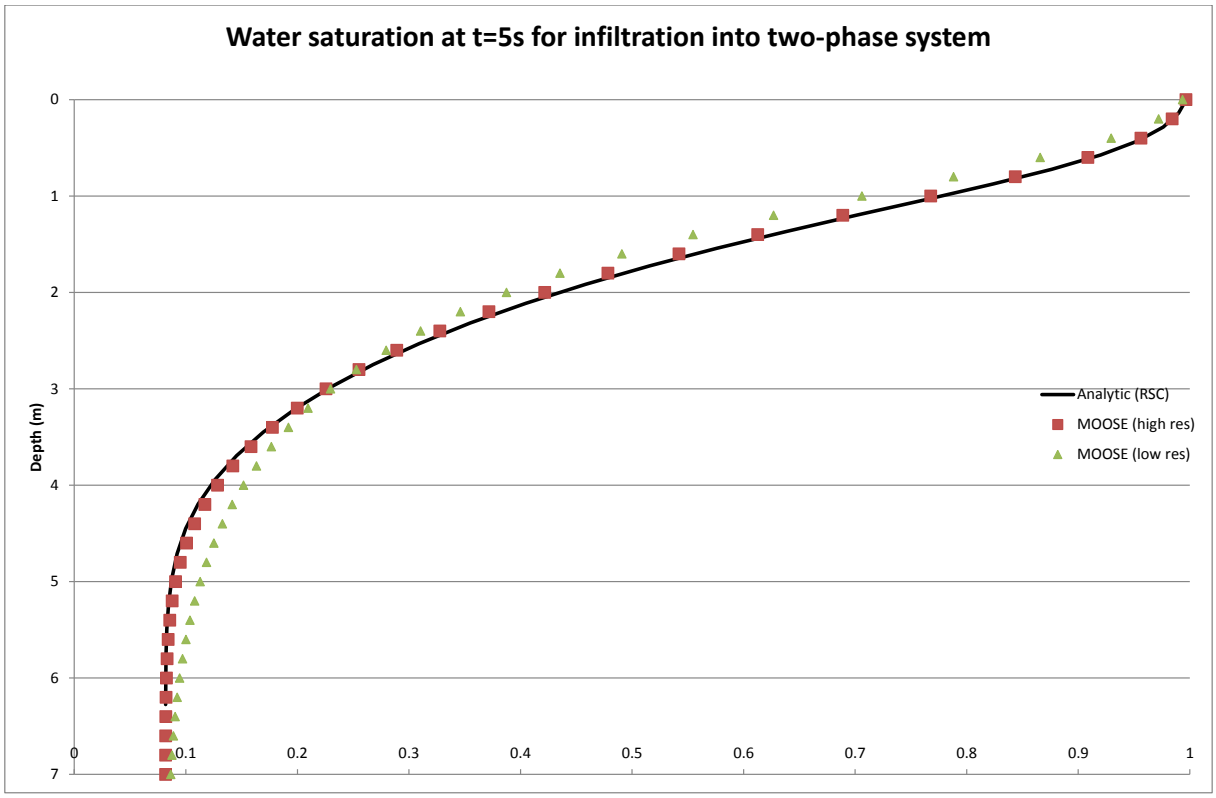

Figure 17.1: Water saturation profile for $t = 5$ s in the Rogers-Stallybrass-Clements test. The initial water saturation is 0.08181, and water is injected at the top of this figure at a constant rate. This forms a water front which displaces the oil. Black line: RSC's analytic solution. Red squares: high-resolution MOOSE simulation. Green triangles: lower resolution MOOSE simulation.

18 The two-phase Buckley-Leverett problem

MOOSE is compared with a simple two-phase one-dimensional Buckley-Leverett problem[1]. The fluids move in a region $0 \leq x \leq 15\,\mathrm{m}$. A water-saturated front initially sits at position $x = 5$, while the region $x > 5$ is initially water-unsaturated. The water pressure is high in the region $x < 5$. With very small capillary suction function $P_c \sim 0$, there is virtually no diffusion of the sharp front, and it progresses towards the right, driven by the high water pressure. This is a difficult problem to simulate numerically as maintaining the sharp front is hard. Moreoever, because it is impossible to use $P_c = 0$ in the MOOSE implementation, it is necessary to use large porepressure changes around the front to create the front. This is difficult to handle numerically. The front's speed is independent of the relative permeability, since the fluid is flowing from a fully-saturated region (where $\kappa_{\mathrm{rel}} = 1$).

In the simulations below, the water pressure at the left boundary is kept fixed at $P_0 = 1\,\mathrm{MPa}$, while the right boundary is kept fixed at $P_{15} = -10^5\,\mathrm{Pa}$. The water viscosity is $\mu = 10^{-3}\,\mathrm{Pa.s}$. In order to correspond as closely as possible to the single-phase version of this test (Chapter 15), the gas-phase viscosity is set to $10^{-6}\,\mathrm{Pa.s}$. This means it interferes very little in the progression of the water front.

The parameters used are listed below

Porosity	0.15
Permeability	$10^{-10}\,\mathrm{m}^2$
Water base density	$1000\,\mathrm{kg.m}^{-3}$
Water viscosity	$10^{-3}\,\mathrm{Pa.s}$
Water bulk modulus	2 MPa
Water relative perm power	2
Water immobile saturation	0.0
Water residual saturation	0.0
Gas base density	$1\,\mathrm{kg.m}^{-3}$
Gas viscosity	$10^{-6}\,\mathrm{Pa.s}$
Gas bulk modulus	2 MPa
Gas relative perm power	2
Gas immobile saturation	0.0
Gas residual saturation	0.0
van Genuchten α	$10^{-4}\,\mathrm{Pa}^{-1}$
van Genuchten m	0.8

[1] SE Buckley and MC Leverett (1942) "Mechanism of fluid displacements in sands". Transactions of the AIME **146** 107–116

The initial condition is

$$P_{\rm water}(t=0) = \begin{cases} 10^6(1-x/5) & \text{for } x<5 \\ -10^5 & \text{for } x\geq 5 \end{cases} , \tag{18.1}$$

and

$$P_{\rm gas}(t=0) = \begin{cases} 10^6(1-x/5)+10^3 & \text{for } x<5 \\ 10^3 & \text{for } x\geq 5 \end{cases} . \tag{18.2}$$

which is shown in Figure 18.1. Using a slighly higher $P_{\rm gas}$ than $P_{\rm water}$ makes the problem more stable, as the gas equations do not vanish in the saturated zeon. With the suction function defined above this gives

$$S(t=0) = \begin{cases} 1 & \text{for } x<5 \\ 10^{-4} & \text{for } x\geq 5 , \end{cases} \tag{18.3}$$

to within 10^{-6}.

The porepressures at the end and right of the model are held fixed.

Good approximations for the water pressure $P(x,t)$ and the front position $f(t)$ may be determined from

$$\begin{aligned} \frac{{\rm d}f}{{\rm d}t} &= -\frac{\kappa}{\phi\mu_{\rm water}}\left.\frac{\partial P}{\partial x}\right|_{x=f} , \\ P(x,t) &= P_0-(P_0-P_f)x/f \quad \text{for } x\leq f , , \end{aligned} \tag{18.4}$$

where P_f is the water porepressure at the front ($P_f=0$) which has solution

$$f(t) = \sqrt{f(0)^2+\frac{2\kappa}{\phi\mu_{\rm water}}(P_0-P_f)t} . \tag{18.5}$$

For the parameters listed above, the front will be at position $f=9.6\,$m at $t=50\,$s. This solution is only valid for zero capillary suction. A nonzero suction function will tend to diffuse the sharp front.

Figure 18.2 shows the results from two MOOSE simulations which validate the MOOSE implementation of two-phase fluid flow. Six simulations in total are part of the test suite:

1. "High res". A uniform mesh of size 0.1 m, with timestep between $10^{-4}\,$s and 0.2 s. The van Genuchten $\alpha = 10^{-4}\,{\rm Pa}^{-1}$ and $m=0.8$. At $t=50\,$s the mesh sits between $x=9.6\,$m and $x=10.2\,$m. One simulation uses SUPG and mass lumping, one uses SUPG and no lumping, and one uses lumping and full upwinding. These simulations use 833 timesteps and take 1 minute to run, so are marked as "heavy" in the test suite and are not run every time the code is updated.

2. "Low res". A uniform mesh of size 0.5 m, with timestep between 0.1 s and 4 s. The van Genuchten $\alpha = 10^{-5}\,{\rm Pa}^{-1}$ and $m=0.8$. Instead of $P=-10^5\,$Pa at the $x=15$ end, $P=-3\times10^5\,$Pa is used instead, which means $s=0.01$ in the unsaturated zone. At $t=50\,$s the mesh sits between $x=9.3\,$m and $x=12.3\,$m. One simulation uses SUPG and mass lumping, one uses SUPG no lumping, and one uses lumping and full upwinding. These simulations uses 37 timesteps and take 0.7 seconds to run, so are part of the automatic test suite.

Mass lumping removes the oscillatory behaviour of the solution, as shown in Figure 18.3.

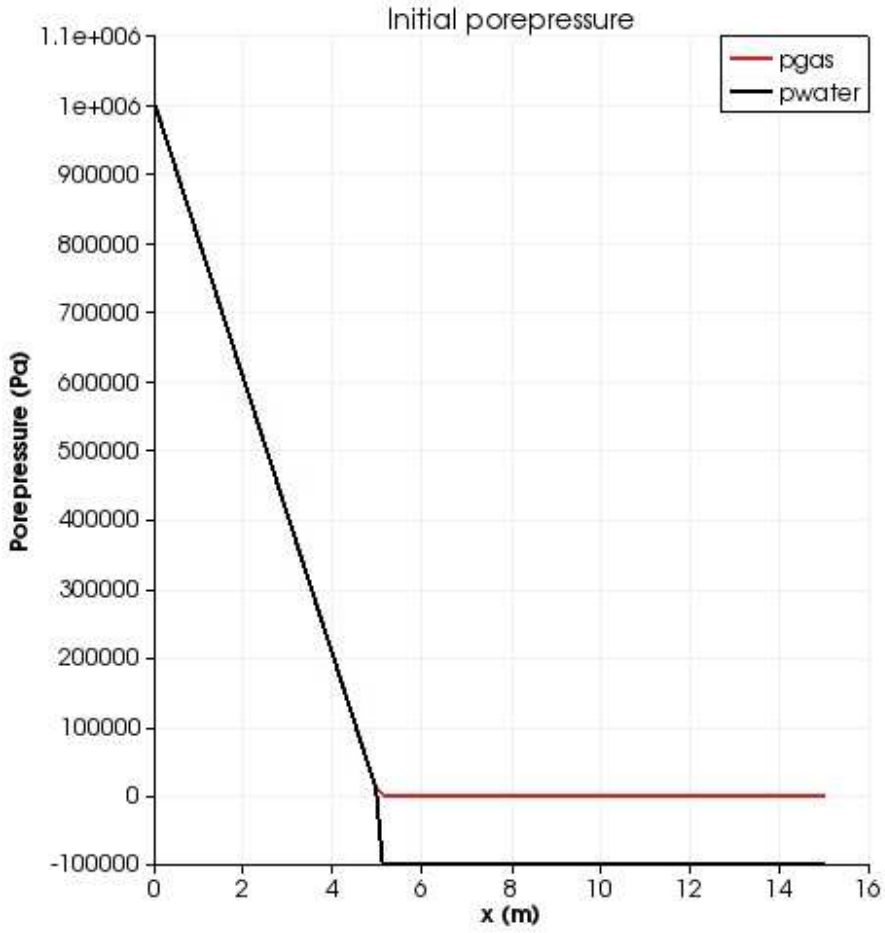

Figure 18.1: Initial setup of the Buckley-Leverett problem where porepressure is a piecewise linear function. The region $x < 5$ is fully water saturated, while the region $x > 5$ has saturation 10^{-4}. During simulation the values of porepressure at the end points are held fixed.

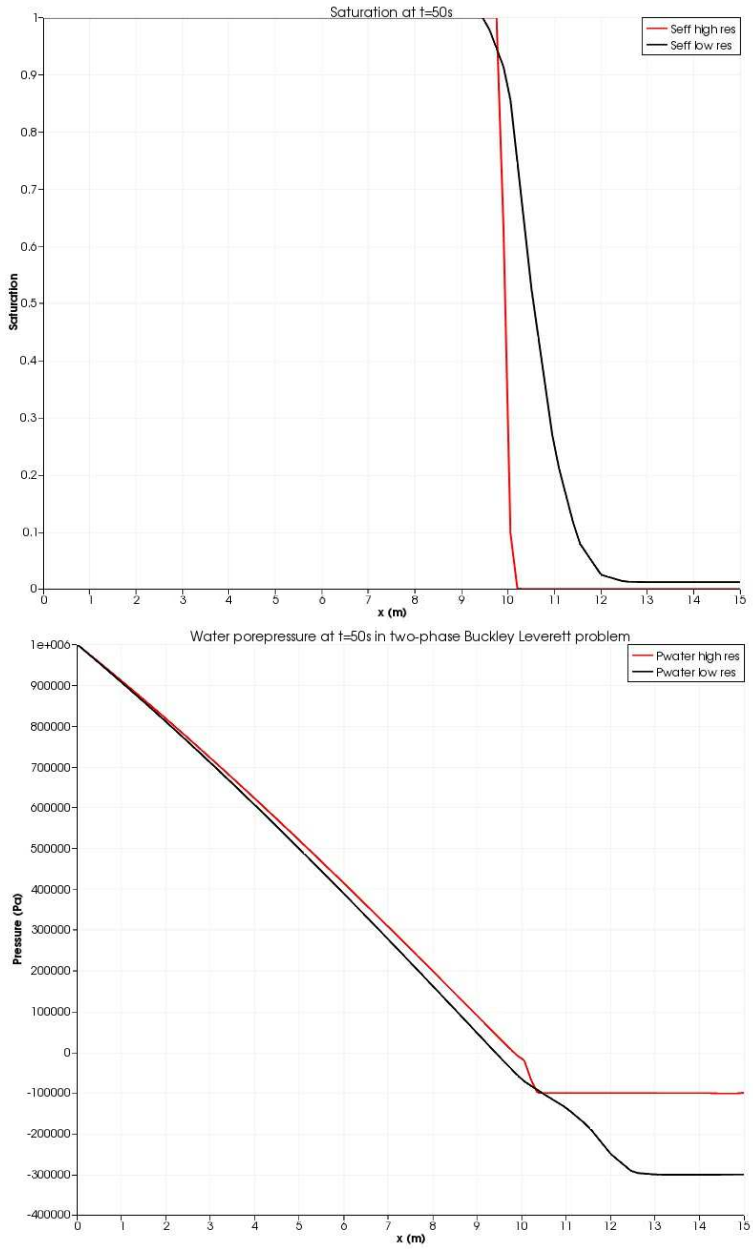

Figure 18.2: The MOOSE solution of the two-phase Buckley-Leverett problem at $t = 50\,\mathrm{s}$. Top: saturation. Bottom: water porepressure. The red line in each is the large $\alpha = 10^{-4}\,\mathrm{Pa}^{-1}$, and the black line is the $\alpha = 10^{-5}\,\mathrm{Pa}^{-1}$. Both these simulations utilise mass lumping.

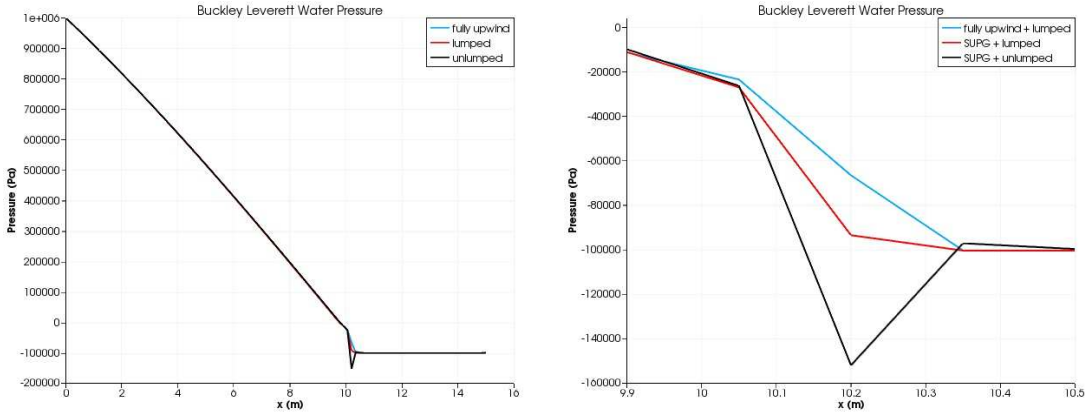

Figure 18.3: Comparison of the two-phase Buckley-Leverett solution at $t = 50\,\mathrm{s}$ with SUPG and no mass lumping, with SUPG and mass lumping, and with full upwinding and mass lumping, for the "high res" case with $\alpha = 10^{-4}\,\mathrm{Pa}^{-1}$. Note the oscillatory behaviour in the unlumped version even though it uses SUPG.